Reply to the Comments of Reviewer #1

We are grateful for your comments. We have already commented on the major issues in the first response “acp-2018-825-response.pdf” from 28th December 2018 where we also explain the strategy for a major revision of the publication.

In the following we will respond to the specific comments (*reprint in italic font*) of the review.

“When the authors explained the motivation of this study, they have claimed that they ‘investigate the mean distribution as well as individual cloud transects’ (L18-19, P2). But looking at individual transects are not meaningful because of the turbulent nature of the environment.”

We are well aware of the turbulent nature of the environment. We agree that the term ‘individual cloud transects’ was misleading and omit this discussion in the major revision. The subsiding shell is now defined by the median distribution of the vertical wind (p4 l28-33)

“That’s why composite analysis of cumulus transects have been conducted in previous works: Wang et al. (2009) over both trade wind and continental Cu, and Katzwinkel et al. (2014) over trade wind ones. Both of those observational studies have performed a more detailed analysis and provided evidence of a subsiding shell at cloud edge based on a large sample of Cu clouds. In my opinion, Section 3 of this manuscript is more like a case study that explains how the clouds and their boundaries are defined.”

Different to earlier works, in the current study we considered only shallow convection over land, captured transects in all cloud levels and included also rather complex clouds (i.e., the clouds can have several updrafts and cloud holes, as long they have a common cloud base). We already discussed the size of our data set in the common response.

A consistent definition of the cloud borders and the methods is given in Sec. 2, while Sec. 3 is indeed a case study in the first place. In the revised paper, we have shortened this chapter. According to the suggestions of Reviewer #2 we have added a thorough analysis of the up- and downdrafts (see Sec. 3.4), which adds a more detailed analysis to the revised paper.

“In addition, the definition of cloud is not consistent in the text. It’s mentioned in the text that the criterion of 100% relative humidity has been used to identify the edges of clouds (Section 2.3). But the cases shown in Figures 5 and 6 are clearly associated with unsaturated air close to at least one identified cloud edge. Apparently, this criterion has not been objectively applied to every sampled cloud and this would significantly impact the results. Take the case shown in Figure 6c as an example. RH does not reach 100% until the x-axis is larger than 0.3. Therefore, I doubt the part of transect (x = [0-0.3]) should be considered as in-cloud region as the authors have done. And the inclusion of clouds incorrectly identified like this would have changed the mean distribution of vertical velocity, buoyancy, and mass flux across the cloud edges”

The definition of the cloud borders and an objective method to select them is taken very seriously in the manuscript. Section 2.3 and especially Table 3 give the applied criteria. Point 3 defines one cloud by the common cloud base, which we verified by the video tape and the operator notes in our analysis. In the concrete example of Fig. 6 c) we agree, that at the first glance the cloud might not start before 0.3 in relative cloud diameter. However, the video tape shows that the narrow cloud fractions indeed belong to the same cloud. Thus, the objective cloud criteria lead to the necessary inclusion of these cloud parts.

We also see the difficulty, that in some cases the cloud gaps are rather big und the structures of the clouds complex. Thus, the analysis is repeated with stricter cloud criteria including only transects with small cloud gaps. The results are discussed in Sect. 4.2 without leading to any significant changes.

“The major portion of the manuscript is based on statistical analysis over 191 identified cloud transects. However, throughout the text, I did not find any texts that have discussed the statistical uncertainty of the shown results. The mean distributions are important. But are they statistically important based on the sample size? In particular, the sample size of the inactive and bottom cases is only 3 in Figure 8, which creates a significant uncertainty when they are compared with other cases.”

In the manuscript we discuss the median distribution and as well their variability by means of the distribution of the 10,25,75,90 percentiles. We agree, that an analysis of the significance should be added to the results where appropriate. We also see the difficulty in interpreting the small sample sizes of the inactive and bottom cases in Figure 8. The reason is very simple; there are not more samples in these classes. They are shown in the figure for reasons of completeness, but we do not draw any further conclusions accepting the lack of significance. We tested the significance of the samples via the bootstrapping method for the revised paper (see p.8 l 29-34) and added this analysis to Fig. 8.

(1) “The authors mentioned that the observed downdraft in the subsiding shell compensates the upward mass flux within the cloud. This conclusion cannot be drawn based on what’s shown. The authors could have tested the validation of the statement by investigating if the updraft in cloud is correlated with the sinking motion around cloud.”

We follow the method of determining the vertical mass flux presented and discussed in earlier publications (e.g., Yang et al. 2016). We see that the method is not explained clear enough and have improved this in the revised version. (p.6 l 25-20 and p.7 l 1-8)

The calculation of the mass flux along a flight path instead of an aerial calculation leads to modified results (Heus et al. 2009). However, it is an appropriate method to understand the air movements in the surrounding of the cloud. In our analysis, we do not set a major focus on the physical numbers of the estimated fluxes, but on the comparability with earlier results and the main consequences on the cloud system. Furthermore, the accumulated mass fluxes are estimated for each individual transect before averaging and thus give indeed information about the correlation of the cloud massflux and the environment.

(2) “The authors should give specific panel numbers to each panel in Figures 6 and 8, and more importantly, refer to figure numbers when discussing relevant findings. I have found the text hard to follow in many places. Examples include but not limited to these paragraphs: L18-27, P6; L17-27, P8.”

We have major interest to improve the readability of the text and figures and therefore have improved the figures and citations in the revised manuscript. We also have improved the mentioned paragraphs.

(3) “*How are the cloud samples stratified to active and inactive subgroups? It’s not clear in the manuscript.“*

The definition is written on page 4 line 3ff and again in the caption of Table 4. In Chapter 2.3 where we define our methods it says: “A further criterion regards the activity status of the cloud, where we request positive mean buoyancy inside the cloud for active clouds.”

(4)” It’s better to change the right axis (RH) to blue colors for easy reading in Figure 6.”

We have changed the colour of the right axis according to the colour of the relative humidity.

(5) „Use consistent units.“

Even though we concentrated also on the consistency of the units, it is possible that we sporadically missed the optimum choice. We have, however, assessed the manuscript in this respect and hope to have encountered all inconsistent units.

Reply to the comments of Reviewer #2

We first of all, thank the reviewer for their thoughtful and detailed comments. We have already commented on the major issues of the review in the first response “acp-2018-825-response.pdf” from 28th December 2018 where we also explain the strategy for a major revision of the publication.

In the following we will respond to the specific comments (*reprint in italic font*) of the review.

“page 1, line 19: would not call this process "simple“; better "this general concept is illustrated in Fig 1..“

We changed accordingly.

p2, l 6: not sure if one can conclude – based on the cited observations - that the subsiding shell does surround the entire cloud. To my opinion, such conclusion can only be drawn from LES

In Heus et al., 2008 (the first cited reference here) the authors define the subsiding shell as a thin coating shell surrounding the cloud, based on LES. However, we agree that in the given context of our measurements this argumentation might be misleading. Therefore, we thank the reviewer to make this point and have adjusted our wording accordingly (i.e., describing the subsiding shell in terms of the mean distribution of the vertical wind as suggested also by Reviewer #1 and discussed in the first response “acp-2018-825-response.pdf”). (i.e., p. 4 l 28 -30)

p2, l 15 to 20: it is not convincing to me that clouds over land should differ from clouds over the ocean with respect to sub-siding shells. I think one should better motivate why the presented observations are novel and one could get new insight in cloud dynamics

We already addressed this point in the first response “acp-2018-825-response.pdf”. The argumentation is changed accordingly in the revised paper (p. 2 l 15-29)

Sec 2.1.& 2.3 One of my main concerns about the observations themselves is the lack of any cloud droplet sensor for a cloud experiment.

We see the advantage of a direct measurement of the liquid water content (LWC) and cloud droplet sensors. It is needed for a calculation of the buoyancy inside the clouds and would also be useful for the investigation of the mixture of cloud and environmental air. We hope to be able to expand the measurement system with such instruments for future research campaigns. The lack of LWC or cloud droplet distribution limited our analysis to the dynamical aspects of shallow convection as discussed in our manuscript.

In terms of the definition of the cloud borders we do not think that a measurement of LWC or cloud droplet numbers is superior to the method presented here. For both alternative measurements we find arbitrary thresholds above zero in literature in order to define the cloud border. This necessarily leads to biases in the cloud border estimation. Furthermore, the reaction time of the sensor is important as well. The Ly-alpha absorption hygrometer used in our analysis measures with 100 Hz and is much faster than most alternatives.

“Another more technical question is if there is a special inlet to avoid droplets entering the Lyman-alpha system, which might influence the readings when leaving the cloud that might bias the data interpretation. I do not generally question the rH measurement

but this should be clarified and/or discussed in detail because it is important. I think for the Lyman-alpha there are better and more fundamental references such as Buck et al."

A modified total air temperature housing is used for the air inlet into the humidity channel. From the inlet a tube is leading the air to the sensors, where also temperature and pressure are measured. The inlet is constructed in a way that first the air of the inlet boundary is separated and second the droplets are separated from the flow through the tube. It is known and discussed in Sect. 2.4.1 of the manuscript (p5 l 9-13) that contamination of the sensors can still occur, which has to be considered. This effect will always lead to an increased humidity mixing ratio and decreased temperature and thus, to increased relative humidity where cloud droplets are present at the sensors. Thus, the influence of cloud droplets inside the cloud will not generate subsaturation. Outside the cloud the influence vanishes very quickly when no sensor wetting occurs.

We have changed the citation according to the suggestion. (p4 l 2)

"It is well known that quite often cumulus clouds are surrounded by almost saturated air (humidity halos) which cannot be distinguished from droplet-free air with your criterion of cloud edges."

Outside the cloud we estimate a measurement uncertainty of the relative humidity of 3% (see Table 1). The regions of almost saturated air (rh > 95 %) are very limited also in the humidity halos. Even within the cloud, relative humidity often goes rapidly down to significant values of subsaturation (e.g., Figures 5 and 6). On the exit side we usually see a clear gradient of the relative humidity even though in some cases the temperature signal might be influenced by evaporation. Thus, the relative humidity is a very good choice to estimate the cloud border.

In the revised paper we now show the median distribution of the relative humidity around the clouds (Fig. 10 panel a). There, indeed the humidity halos are visible, but also the very narrow regions of almost saturated air.

Sec 2.2: At some point it would be essential to get more information about the sampled cloud fields, e.g. cloud base height and cloud tops, temperature and so on. From this information one could at least estimate the adiabatic LWC, which give us a range for the liquid water mixing ratio and, therefore, the maximum error for the calculated buoyancy.

We agree on that and have included this information in the revised manuscript. We understand that this additional information has an important value for the reader. We have added the information about the sampled cloud fields to Table 2 in the manuscript which lists the measurement flights of the campaign. The influence on the buoyancy is now discussed in Sec. 2.4.2.

P4, l12: Please discuss a little bit more in detail why you didn't simply applied criteria used for previous observations. This would have the advantage to better compare the results with each other. You should have good reasons to introduce new criteria!

We have addressed this point with a close look at the previous observations. This is indeed important for the cloud definition. However, the definition of the subsiding shell is still limited to the median distribution, while we refrain from investigating the individual transects - as suggested by the reviews. The respective discussions in the new manuscript are at p. 4 l 4-17 f or the cloud definition and at p. 4 l 22-33 for the subsiding shell)

Sec 2.4.2 "LWC – in particular for non-adiabatic regions such a cloud boundaries is a highly fluctuating parameter. To assume a constant value is a very strong simplification. Please discuss in detail the consequences and a maximum error for the derived buoyancy. Without such a discussion the presented buoyancy is highly questionable. I suggest ignoring the LWC and discussing the maximum error for B; this might be more straightforward compared to use a constant value for LWC – the error will be small and not alter your results. The variation of LWC as seen in Wang et al describe more the deviation from the adiabatic LWC which itself is a function of height and cloud base temperature."

The influence on the buoyancy is now discussed in the respective section (p6 l 9-16). We calculate the adiabatic LWC gradient from the measured profile data during the flights and as suggested give an estimation of the maximum errors. We have also followed the suggestion to show the buoyancy calculation without the LWC influence in Fig. 10 c).

Discussion, line 23ff: "You mentioned that a certain fraction of the sampled clouds do not show a subsiding shell on both sides. Based on this finding I have serious concerns how representative an estimated mass flux distribution is? One should remember that a flight through a cloud is one single realization and more a "spaghetti-like" penetration."

Indeed, the calculation of the vertical mass flux along the flight path leads to a difference when compared to the aerial calculation, which are possible with LES models (Heus et al. 2009). However, it is a common method also described in earlier publications (e.g., Yang et al., 2016). A single realization of the mass flux as determined in our paper is certainly not representative for 'a cloud', but averaging (over many spaghetties) should at least provide an estimate of the potential magnitude and direction. This is also important for the cloud properties in Figs. 7 and 10 where we only show the statistical distributions (i.e., the medians and percentiles). On the reviewer's suggestion we have emphasized this more (and hopefully better) in the revised manuscript.

Our conclusion of the calculation describes a significant contribution of the compensating vertical mass flux in the near surrounding of the cloud. This is in concordance with the LES results even though we find it to be the result of the elevated frequency of downdrafts in the vicinity of the clouds.

P11, line 1 "We find a positive correlation of vertical wind and buoyancy (i.e., r _ 40%). Near the cloud gaps this indicates mixing of cloud air with environmental air" I cannot follow this logic; the first part of this statement simply states that about 40% of the data shows an actively growing cloud (following Katzwinkel's nomenclature) but how can you conclude that this means mixing around cloud gaps? Cloud gaps are most probably the consequence of mixing. Please explain your conclusion. The intention of next statement is also not clear; it is the nature of turbulence that up- and downdrafts can be observed close to each other so why should one be surprised to find this in cumulus clouds? Maybe this is simply a misunderstanding on my side"

We have modified the argumentation in the revised manuscript (p 12 l. 34ff).

P11, l12" On the downwind side of active clouds the broad region of downdrafts is explainable by a humidity halo as observed by Perry and Hobbs (1996). Why can broad regions with downdrafts be explained by humidity halos. By the way, if you cannot measure

LWC but instead define your cloud boundary by relative humidity you cannot identify humidity halos, which are characterized by almost saturated conditions but no cloud droplets."

We agree, that this needs further explanation. As discussed above, there is a small chance that we assume a cloud where already the region of a humidity halo has started, but not the opposite way. Therefore, when we measure enhanced humidity compared to the environment we can detect this region. The humidity halo is seen as a mixture of cloud and environmental air. Therefore, it can have significant subsaturation and enhanced humidity. The evaporation of the cloud droplets leads to cooling and negative buoyancy (p9 l 15-19, p12 l 27-34). The correlations of buoyancy and vertical wind in the analysis of the downdrafts have been calculated and added (Table 7) to support these conclusions.

"It was quite often concluded that your observations are similar to previous observations – so the reader is left with the question "What is new in your study?'
'An investigation of size, turbulence statistics and scaling with the cloud size in future research is desirable to understand the dynamics of shallow convection over land.'
Why not starting with answering these questions in this paper?"

We have adopted this suggestion and expanded the revised manuscript by the analysis of the up- and downdrafts in the vicinity of the clouds (Sec. 3.4). We hope that this has added a valuable additional and new apsect to the revised paper.

References

Heus, T., C. F. J. Pols, H. J. J. Jonker, H. E. A. Van den Akker, and D. H. Lenschow, 2009: Observational validation of the compensating mass flux through the shell around cumulus clouds. *Quarterly Journal of the Royal Meteorological Society*, **135 (638)**, 101/112, URL http://dx.doi.org/10.1002/qj.358.

Katzwinkel, J., H. Siebert, T. Heus, and R. A. Shaw, 2014: Measurements of turbulent mixing and subsiding shells in trade wind cumuli. *J. Atmos. Sci.*, **71 (8)**, 2810/2822, URL http://dx.doi.org/10.1175/JAS-D-13-0222.1.

Perry, K. D., and P. V. Hobbs, 1996: Influences of isolated cumulus clouds on the humidity of their surroundings. *J. Atmos. Sci.*, **53 (1)**, 159/174, URL http://dx.doi.org/10.1175/1520-0469(1996)053*h*0159:IOICCO*i*2.0.CO;2.

Stevens, B., and G. Feingold, 2009: Untangling aerosol effects on clouds and precipitation in a buffered system. *Nature*, **461 (7264)**, 607{613, URL http://dx.doi.org/10.1038/nature08281.

Wang, Y., B. Geerts, and J. French, 2009: Dynamics of the cumulus cloud margin: An observational study. J. Atmos. Sci., 66 (12), 3660/3677, URL http://dx.doi.org/10.1175/2009JAS3129.1.

Yang, J., Z. Wang, A. J. Heymsfield, and J. R. French, 2016: Characteristics of vertical air motion in isolated convective clouds. *Atmospheric Chemistry and Physics*, **16 (15)**, 10 159{10 173, URL http://www.atmos-chem-phys.net/16/10159/2016/.

Subsiding shells and ~~vertical mass flux~~ the distribution of up- and downdrafts in warm cumulus clouds over land

Christian Mallaun[1], Andreas Giez[1], Georg J. Mayr[2], and Mathias W. Rotach[2]

[1]Deutsches Zentrum für Luft- und Raumfahrt (DLR), Flight Experiments, Oberpfaffenhofen, Germany
[2]University of Innsbruck, Institute of Atmospheric and Cryospheric Sciences, Innsbruck, Austria

Correspondence to: Ch. Mallaun
(christian.mallaun@dlr.de)

Abstract. The mass flux of air lifted within the updrafts of shallow convection ~~was~~ is usually thought to be compensated outside the cloud through either large scale subsidence or stronger downdrafts in a thin shell surrounding the cloud. Subsiding shells were postulated based on large eddy simulation and are experimentally tested in this study for shallow convection over land. Isolated cumulus clouds were probed with a small research aircraft over flat land ~~, mountains,~~ and mountainous terrain, in different wind situations and at different levels of the clouds. The ~~subsiding shell varies considerably between individual cloud transects. A shell-like narrow downdraft region was present on at least one edge in 105 out of~~ average of the 191 ~~transects and on both edges in 29 transects. However, the average over all~~ cloud transects shows the subsiding shell as a narrow downdraft region outside the cloud boundaries. The ensemble-mean subsiding shell is narrower on the upwind side of the cloud, while it is at least half a cloud diameter wide and more humid on the downwind side. At least half of the upward mass transport in the cloud is compensated within a distance of 20 % of the cloud diameter. ~~A~~ However, this shell is not uniform. Distinct regions of downdrafts and updrafts with high variability of the vertical wind are frequent and randomly distributed in the vicinity and also within the cloud. ~~Based on these findings, a subsiding shell is , however, a valid concept to describe an ensemble of shallow cumulus clouds over land.~~ The median diameter of the drafts directly at the cloud boundary is at least 4 times as large as inside the clouds and in the environment. Downdrafts at the cloud boundary are twice as frequent as updrafts. In contrast to the updrafts the major part of the downdrafts is situated outside of the cloud. The subsiding shell results from the distribution of these up- and downdrafts.

1 Introduction

Air in shallow cumulus clouds is transported towards higher regions of the atmosphere where it detrains from the cloud and mixes with environmental air. This is an effective way to vertically transport energy, heat and moisture from the surface to higher levels. Traditionally, large scale subsidence between the isolated cloud cells is regarded to be responsible for compensating the mass flux within the cloud (e.g. Stull, 1988). Heus and Jonker (2008) found a characteristic thin layer of a downward airflow outside of the simulated cumulus clouds by means of Large Eddy Simulations (LES), which they named the subsiding shell. This ~~simple cloud process is sketched~~ general concept is illustrated in Fig. 1.

A similar concept already appears in the cloud model of shallow cumulus clouds by Scorer and Ludlam (1953). They describe a region of downward motion in the wake of a rising bubble, which is caused by evaporation of the cloudy boundaries. With respect to the turbulence in the cloud they conclude, that the disturbances within the undiluted updrafts might be small compared to the wake region where violent eddies are dominating. Jonas (1990) found such significant downdrafts outside of growing cumulus clouds from airborne measurements, while these were missing in the decaying clouds. This is also confirmed by later measurements (e.g. Rodts et al., 2003; Blyth et al., 2005).

Wang et al. (2009) investigated the mean dynamical properties of the cloud margin in shallow convection with a large number of cloud transects from aircraft measurements and confirm the subsiding shell as a distinct minimum of vertical velocity at the cloud boundaries. Mixing of cloud and environmental air leads to evaporative cooling, which is the source for the subsiding shell (Heus and Jonker, 2008; Abma et al., 2013; Katzwinkel et al., 2014). Even though the subsiding shell is rather thin, the covered area is significant as it surrounds the entire cloud (Heus and Jonker, 2008). Therefore, the area of the shell is large enough to account for major parts of the downward mass flux in the cloud free environment, while the contribution of subsidence outside of the shell is less important. Jonker et al. (2008) calculated the fraction of mass compensation to be $80\,\%$ within a diameter of $400\,\mathrm{m}$ around a cumulus cloud. The ability of the clouds to condition the entire atmospheric boundary layer (ABL) is strongly reduced by these downdrafts. Additionally, ~~it is~~ they are an efficient way to bring air from the top of the cloud to its lateral boundaries, where it can entrain into the cloud. Consequently, this entrained air has properties from above the entrainment level. Wang and Geerts (2010) showed that the thermodynamic properties of the air in the vicinity of the cloud vary strongly with its horizontal distance from the cloud.

Most measurements discussed so far targeted shallow convection above the ocean (e.g. Heus and Jonker, 2008; Jonas, 1990; Katzwinkel et al., 2014), although this cumulus cloud type is also a common and characteristic phenomenon in the temperate and continental climate of the mid-latitudes. The measurements of Katzwinkel et al. (2014) were restricted to the top level of the investigated maritime cumuli because of system limitations. They investigated the individual updrafts at the cloud top and therefore found mostly small clouds. Wang et al. (2009) included shallow convection over land in their analysis ~~, but restricted themselves to~~ and investigated the mean properties of the cloud ensemble. Many of their convective clouds over land were containing rain and ice particles with cloud tops usually well above $4\,\mathrm{km}$. In this study, we present the results of 6 measurement flights over central Europe to test the validity of the subsiding shell ~~concept for shallow convection over land.~~ to further detail over different types of land characteristics (flat versus mountainous terrain). The cloud transects were flown at different height levels, directions as well as during different synoptic situations. Thus, the analysis is limited to cumulus humilis and mediocris, but allows for a comprehensive picture of these cloud types. We investigate the ~~mean distribution as well as~~ dynamical properties of these clouds with a special focus on the cloud borders looking for the subsiding shell. Due to the turbulent character of the cloud system the subsiding shell can only be detected in the mean distribution of the vertical wind near the cloud boundaries. As the individual cloud transects ~~and discuss shallow convection for different synoptic situations and terrain~~are known to include strong up- and downdrafts within the cloud (Yang et al., 2016), we expand the analysis of these drafts to the cloud boundaries and the near environment, so as to understand the structure of the subsiding shell.

In the following section we describe the assets and limitations of the instrumented aircraft and give an overview of the measurement campaign and methods. In Section ~~3.1 we show~~ 3 we present the results for some selected cloud transects~~and look at~~

~~the distribution of the wind and thermodynamic properties of the individual cloud transects~~. This is followed by more general observations of the mean properties and variability of shallow cumulus clouds~~and especially~~ , the characteristics of the subsiding shell ~~in Sect. 3.~~ and the distribution of up- and downdrafts. We discuss the importance of the subsiding shell with a focus on the downward mass flux and the statistics of the drafts in Sect. 4, before we end with the conclusions in Sect. 5.

2 Probing shallow convection and the subsiding shell

2.1 The research aircraft

For the in situ measurements we used a Cessna Grand Caravan 208B (Caravan), which is equipped with a meteorological sensor package (Mallaun et al., 2015). This small research aircraft combines several advantages for the investigation of small scale phenomena in the ABL such as the strong single engine power, high manoeuvrability and robust design. It is equipped with a high accuracy inertial reference system (IRS) for position and attitude determination and a meteorological sensor package mounted under the left wing. Mallaun et al. (2015) describe the details of the measurement instrumentation and the corresponding uncertainties for the high-frequency 100 Hz measurements of pressure, temperature, humidity and wind vector. The main results of the measurement accuracy are summarized in Table 1.

2.2 The measurement campaigns

We conducted 6 measurement flights during two campaigns in June 2012 and July 2013 as listed in Table 2. Flights 1, 2 and 6 were conducted over relatively flat terrain north of the Alps and west of Munich (D), with smooth hills covered by fields and woodland. On the first two flight days high pressure influence was dominating. The wind and wind shear were moderate from western direction during flight 1 and very weak during flight 2. Examples for the clouds during the first two flights are shown in Figure 2. During flight 6 the wind was moderate from north-west and in the rather humid surrounding ($rh > 70\,\%$) the cloud cover was higher and the cumulus clouds were situated in lower levels compared to the other flight days. Flights 3 to 5 were devoted to the investigation of convective clouds over alpine ~~topography. The~~ orography. The clouds developed above the mountain peaks during strong high pressure influence with weak southerly wind. The convection tended to start above distinct points above the mountain ridges drifting north during its life cycle. The flight tracks are shown in Figure 3 and information about the flight conditions can be found in Table 2.

We chose a similar flight strategy for all flights in order to achieve comparable data sets. Each flight started and ended with a vertical profile to obtain information about the undisturbed atmosphere outside the cloud. During ascent the cloud base and top were defined visually and a mean wind direction was estimated from the on-board quicklook data. With this information the operator defined the flight directions ~~along and across the~~ 'along' and 'across' the mean wind and up to three height levels within the cloud. In some cases also transects below cloud level were flown. Figure 4 shows the definitions of flight levels and directions as well as the main flight pattern, which is shaped like an 8. We also performed a simple reverse heading pattern, which allows for a high transect rate and facilitates the relocation of the target cloud. Beside the single cloud sampling we also performed longer straight flight legs in different directions and levels in order to gain broader statistics of the cloud properties.

2.3 Identifying clouds

The target clouds were selected visually during the flight. The identification of the cloud boundaries is realized in two steps. First, a digital time mark set by the operator during the flight gives a rough estimate of the location. As a second step, we take the signal of relative humidity to determine the exact cloud boundaries. Thus, *the cloud starts and ends with humidity saturation* as measured by a Ly-α absorption hygrometer ~~(e.g. Bange et al., 2002)~~(Buck, 1976), which has a response time faster than the acquisition frequency of $100\,\mathrm{Hz}$.

We request a cloud diameter of at least $200\,\mathrm{m}$ to avoid very small cloud filaments. Such a cloud transect typically includes about 300 data points. This limit left us with 191 cloud transects including 17 different individual clouds which were repeatedly penetrated. Other authors have required different minimum cloud lengths. The scarce resolution of models or earlier measurements required higher thresholds of $\approx 500\,\mathrm{m}$ (e.g., Heus and Jonker, 2008; Jonas, 1990). More recent measurements, for example Wang et al. (2009) request a minimum length of $200\,\mathrm{m}$~~or Katzwinkel et al. (2014)~~, or Katzwinkel et al. (2014) one of $50\,\mathrm{m}$.

Several factors complete the identification of a cloud. A single cloud often consists of more than one updraft. It can contain large gaps above its base, which makes it difficult to distinguish it from other clouds in the vicinity. Figure 2 a) shows an example. The cloud consists of an active updraft near the upwind side of the cloud separated by a gap at higher levels from an older, already decaying updraft further downwind, but joined through a common cloud base. For the data evaluation, we have used the flight protocol and video tape to confirm the common cloud base. We also use a subset of 94 transects for which gaps in the transects above common cloud base were at most $150\,\mathrm{m}$ and less than $30\,\%$ of the cloud diameter. The cloud definition is summarized in Table 3. The existence of cloud gaps is in line with recent measurements (e.g. Jonas, 1990; Blyth et al., 2005; Wang et al., 2009; Katzwinkel et al., 2014). The detection of the common cloud base it hardly possible with a fully automatic cloud analysis, but inevitable with our observations during the measurement campaign.

We classified the cloud transects in terms of cloud region (bottom, middle, top), along- or crosswind transects and terrain (lowland, mountains). A further criterion regards the activity status of the cloud, where we request a positive ~~mean~~ median buoyancy inside the cloud for active clouds. The numbers of selected cloud transects representing the different criteria are listed in Table 4.

No agreement exists what constitutes a subsiding shell. Heus and Jonker (2008) originally defined a $50-100\,\mathrm{m}$ range of negative vertical wind directly outside the cloud. Wang et al. (2009) use a range of $50\,\mathrm{m}$ within and $200\,\mathrm{m}$ outside the cloud. Katzwinkel et al. (2014) split the subsiding shell in an inner and outer shell, where the inner shell has negative vertical velocities and negative buoyancy. It is driven by the negative buoyancy after mixing and evaporation at the cloud boundary (Abma et al., 2013) and thus, can partially also appear inside the cloud. The outer shell has still negative vertical velocity but positive buoyancy. ~~Based on these ideas we used the following criteria to identify a subsiding shell : In order to capture a high number of cases the width of the subsiding shell must be between 1 % and 20 % in cloud diameter. A downdraft exists within 5 % in cloud diameter outside of the cloud boundary. The subsiding shell can already start within the cloud. However, it must not have~~

~~a length of more than $20\,\%$ in cloud diameter. This definition is summarized in Table 3. The median cloud length of the 191 transects is $\approx 1300\,\mathrm{m}$. Thus, the median subsiding shell has a length between $13\,\mathrm{m}$ and $260\,\mathrm{m}$ and starts within $65\,\mathrm{m}$ outside the cloud boundary. A possible part of this downdraft region inside the cloud is not longer than $260\,\mathrm{m}$. The length~~ Generally, the existence of the subsiding shell is identified by a negative peak of the mean (or median in a non-Gaussian process) vertical velocity right outside the cloud boundaries. Due to the turbulent character of the cloudy environment a single representation of a cloud transect will usually not exhibit the characteristics of a subsiding shell. The mean distribution of the vertical velocity gives insight in the strength and depth of the subsiding shell. We investigate the width of the shell relative to the cloud diameter which accounts for the ~~high~~ strong variability of cloud size. A circular subsiding shell with a ~~length~~ width of $20\,\%$ in cloud diameter has an area approximately equal to the embedded cloud.

In order to assess the structure of the subsiding shell we analyse the properties of the up- and downdrafts in the vicinity of the cloud. In accordance with Yang et al. (2016) we define a downdraft (updraft) as the region where the vertical velocity is below $-0.2\,\mathrm{ms}^{-1}$ (above $+0.2\,\mathrm{ms}^{-1}$). The small deviation from zero accounts for small-scale turbulence inside the up- and downdrafts and also corresponds to the measurement uncertainty of the system. Thus, regions with small vertical velocity are disregarded. We omit up- and downdrafts narrower than $10\,\mathrm{m}$. Furthermore, where the gap between two neighboring downdrafts (updrafts) is smaller than $10\,\mathrm{m}$ and the vertical wind does not exceed $+0.2\,\mathrm{ms}^{-1}$ (fall below $-0.2\,\mathrm{ms}^{-1}$) the up- or downdraft is considered as a single one. They are estimated for the cloud region and up to 0.5 cloud diameters away of the cloud boundary. Three different categories of up- and downdrafts are distinguished: inside the cloud, at the cloud boundary and in the environment. The up- or downdraft at the cloud boundary are situated partly inside *and* outside the cloud.

2.4 Computation of derived variables

2.4.1 Corrections of measurements in clouds

The presence of liquid water in the cloud modifies temperature and humidity measurements. Some of the liquid water evaporates as air is compressed in and in front of the total air temperature housing reducing the static temperature (T_s) and increasing the humidity mixing ratio (r) and thus the dewpoint temperature (T_d). We can estimate $T_d - T_s$ as the sum of evaporative cooling (ΔT_s) and the increased dewpoint temperature (ΔT_d) with

$$T_d - T_s = \Delta T_s + \Delta T_d = \frac{L_h \cdot \Delta r}{c_p} + \frac{\partial T_d}{\partial r} \cdot \Delta r, \tag{1}$$

as long as no significant sub- or supersaturation is present inside the cloud. The bias in water vapour mixing ratio (Δr) is equal to the evaporated amount of cloud water. In this approximation we use $L_h = 2.5\,\mathrm{MJkg}^{-1}$ for the standard enthalpy of evaporation and $c_p = 1005\,\mathrm{JK}^{-1}\mathrm{kg}^{-1}$ for the heat capacity at constant pressure. The change of dewpoint temperature with the change of mixing ratio ($\partial T_d / \partial r$) depends on pressure and temperature.

The humidity mixing ratio correction can be computed from Eq. 1,

$$\Delta r \approx (T_d - T_s) / \left(2.5\,\mathrm{K\,g^{-1}\,kg} + \frac{\partial T_d}{\partial r} \right), \tag{2}$$

if the mixing ratio is expressed in $\mathrm{g\,kg^{-1}}$, where $(T_d - T_s)$ is measured and the value for $\frac{\partial T_d}{\partial r}$ is calculated individually for each flight as listed in Table 5 following the common approximations for humidity conversion (e.g. Stull, 2000). The evaporation of Δr causes a cooling of the static temperature (ΔT_s) of

$$\Delta T_s = \frac{L_h \cdot \Delta r}{c_p} \approx 2.5\,\mathrm{K\,g^{-1}\,kg} \cdot \Delta r. \tag{3}$$

This correction rarely exceeds $1\,\mathrm{K}$ for the temperature and $0.4\,\mathrm{gkg^{-1}}$ for the mixing ratio.

However, when sensor wetting occurs as described by Lawson and Cooper (1990) and Wang et al. (2009), a cold peak can cause significantly larger errors especially outside the cloud and this correction does not work. On the Caravan two redundant temperature sensors (identical in construction) were available, which show different sensor wetting and thus, also different amplitudes of the cold peak. This allows for a very simple detection of the wetting effect. Consequently, for the investigation of the potential temperature and buoyancy distributions we have used just the first half of the transects in order to minimise the impact of sensor wetting. As the transects can start on either side of the cloud, the median distributions are available for the entire cloud transects, but contain a reduced set of data. The cold peak was often not visible in our measurements and the corrections defined in Eqs. 2 and 3 are applied to all data.

2.4.2 Computation of ~~the~~ buoyancy

The buoyancy is determined according to

$$B = g\left[\frac{\Theta_v'}{\overline{\Theta_v}} + (1-\kappa)\frac{p'}{\overline{p}} - 10^{-3} r_l\right], \tag{4}$$

(Eq. 2.52, Houze (2014)) . To ~~calculate~~ determine the virtual potential temperature (Θ_v) in clouds, the ~~LWC~~ liquid water content (LWC) is additionally needed (i.e., $\Theta_v = \Theta(1 + 0.61 \cdot 10^{-3} r - 1 \cdot 10^{-3} r_l)$, with the liquid water mixing ratio (r_l) (Stull, 2000). Again, r and r_l are expressed in $\mathrm{g\,kg^{-1}}$. ~~The~~ Since the LWC is not measured directly, ~~thus, for the calculation we assume a value of $r_l = 0.4\,\mathrm{gkg^{-1}}$~~ we omit this effect in the calculation, which introduces a positive bias within the clouds. However, this bias will be small for the shallow cumulus clouds especially at the cloud boundaries where we find the region of our special interest. In order to estimate the bias, we calculated an adiabatic value of LWC as the difference of the saturation humidity mixing ratio at the measurement height and the cloud bottom. We estimated an increase of the LWC to be $dLWC \approx 2\,\mathrm{gkg^{-1}km^{-1}}$ for the ~~regions with humidity saturation, which corresponds to a temperature difference of $\sim 0.15\,\mathrm{K}$. The results of Wang et al. (2009) indicate smaller values of LWC near the cloud margins and slightly higher ones in the updraft core.~~ measurement flights described in Sec. 2.2. Only for flight 6 it was smaller with $dLWC \approx 1.6\,\mathrm{gkg^{-1}km^{-1}}$. According to Warner (1977) the true LWC is much smaller and will rarely exceed $r_l = 1\,\mathrm{gkg^{-1}}$. Thus, also the contribution to the buoyancy is small.

Similar to Wang et al. (2009), we calculate the mean values ($\overline{\Theta_v}$) and mean pressure ($\overline{p}$) from the data of each cloud transect. The perturbation values (Θ_v', p') are then defined as the deviation from these mean values. ~~Here~~In Equation 4, κ is the ratio of the gas constant and the specific heat capacity of air at constant pressure (i.e., $\kappa = R/c_p = (c_p - c_v/c_p)$) and g the acceleration due to gravity. The conserved variable Θ_v is used to compensate for inevitable height changes of the aircraft during the passage through the cloud. The pressure is altitude-corrected as described in Mallaun et al. (2015) with

$$p_{\text{ref}} = p_0 \cdot e^{-\frac{g \cdot \Delta h}{R \cdot \overline{T}_v}}. \tag{5}$$

For p_0 we take the pressure at the starting point and $\overline{T_v}$ is the mean value of virtual temperature approximated by the mean values at the current position and the starting point, Δh is measured with the DGPS.

2.4.3 Computation of the vertical mass flux

In order to calculate the mean vertical mass flux (f_m) from the center of the cloud to the cloud boundary and the compensating downward directed mass flux outside of it, we adopt the formulation presented in Yang et al. (2016). From the flight data only the mass flux along the flight track can be estimated, the differences compared to an areal approach are discussed in Heus et al. (2009). We calculate the vertical mass flux for the ~~relative~~ distance (x) from the cloud boundary with

$$f_m(x) = \rho(x) \cdot \cancel{n} w(x) \cdot \mathrm{d}x. \tag{6}$$

$w(x)$ is the vertical velocity at ~~a relative distance~~ the position (x) ~~from the cloud boundary and ρ~~ and $\rho(x)$ the air density~~, the overbar denotes the mean value of all data points with a common x for the density and wind product. Thus, $x = 0$ is at the boundary, positive values are within the cloud with a maximum of $x = 0.5$ at the center of the cloud and negative ones in the surrounding shell. $n(x)$ represents the number of data points within the range of x~~. The accumulated mass flux (F_m)

$$F_m(x) = \int_{\cancel{0.5}\,x_0}^{\cancel{x}\,x} f_m(x')\,\mathrm{d}x' \tag{7}$$

measures the integrated upward flux of air inside the cloud and estimates the compensating downward mass flux outside. The limits of integration ~~reach~~ range from the cloud center x_0 to x. In our analysis we consider only relative values of $f_m(x)$ and $F_m(x)$, which are scaled by their respective maximum values. Also the horizontal distance x is scaled to the individual cloud length. Thus, the smaller clouds have the same statistical weight as the big clouds when the averages for all the cloud transects are calculated.

3 ~~The~~ Properties of the cumulus clouds and the subsiding ~~shell in single cloud transects~~shells

3.1 ~~The subsiding shell in an example cloud of a low-wind flight~~

Altogether, we investigated 191 cloud transects for the measurement flights described in Sec. 2.2. The clouds are selected according to the cloud definition in Table 3 and results in 94 transects when the stricter criteria are applied. An overview on the numbers for the different transect classification is given in Table 4. All these transects build a large sample to investigate the statistical distribution of the characteristic cloud properties. The boundaries of the clouds are estimated by the humidity distribution. Thus, the dynamical properties in the focus of the following discussion are independent of the cloud definition. First, we look at a series of particular cloud transects during flight 2. This helps to explain the methods ~~and~~ as well as to discuss the cloud characteristics and the ~~occurrence of the~~ subsiding shell for the chosen examples. ~~On the flight day~~

3.1 The vertical wind distribution in individual cloud transects

During the day of flight 2 shallow convection formed around midday in a low-wind situation with weak high pressure influence. Compared to the other flight situations the horizontal wind and wind shear of $\approx 1\,\mathrm{ms^{-1}km^{-1}}$ were very weak - at least up to the highest flight level. ~~-~~Some meteorological parameters of the environmental air are listed in Table 2.

Figure 2 a) shows an example cloud of this flight including a narrow cloud turret, which grew fast above the broader and longer persisting cloud base. After $5-10\,\mathrm{min}$ the turret (the upper part of the cloud) dissolved in the relatively dry surrounding air and gave way to a new updraft, while the cloud base persisted. ~~Figure 5 a)~~

Figure 5 shows measurements along a crosswind transect flown in the upper part of another cloud ~~.~~ during flight 2. The relative humidity in panel a) shows a compact cloud with small cloud gaps in the western part indicated by subsaturation. Here, also the vertical wind velocities (panel b) are small compared to the eastern half where updrafts of up to $5\,\mathrm{ms^{-1}}$ are present. Also the buoyancy shown in panel c) is increased in the updraft region, while the pressure perturbation in panel d) is significantly negative in the dissolving (or decaying) part of the cloud.

Outside the cloud boundaries, a clear signal of sinking air with magnitudes up to $3\,\mathrm{ms^{-1}}$ is present. On the left boundary an $\approx 200\,\mathrm{m}$ wide region of downdrafts starts already within the cloud. ~~This is the subsiding shell.~~ On the right side the downdraft region is $\approx 300\,\mathrm{m}$ wide with a distinct minimum about $150\,\mathrm{m}$ away from the cloud boundary followed by a weak subsidence region. ~~However, not all of the transects possess a~~ It is important to note, that due to the turbulent character of the cloudy environment the representation of a single cloud transect cannot give a distinct information about the existence of the subsiding shell. ~~Figure~~

Not many of the investigated individual transects possess such distinct downdrafts directly outside of both of the cloud boundaries. For example, Fig. 6 shows humidity and vertical wind for 4 different transects for the same cloud in north-south direction (along the main wind direction). From the video tape and operator's notes there is strong evidence that all cloud parts have a common base, even though rather large sub-saturated regions occur ~~. These~~ (e.g., Fig. 6 c). Such gaps occur very frequently when weaker decaying cloud parts and regions with stronger updrafts tend to line up along the mean wind direction. It is almost impossible to recognise the vertical wind structure from one transect to the other, which ~~might be due to a~~ is due to the turbulent nature and the high spatial /temporal variability and transient behaviour of the ~~cloud. In~~ flow in the cloud. Apparently, not even the updraft (downdraft) regions can be identified as quasi-steady 'coherent structures' as is sometimes the case in small-scale turbulent flows. However, in panel c) and d) the main updraft might be the same, but for the rest of the transects the vertical velocity structures are different. This is similar for many transects in other clouds (not shown).

Figures 5 and 6 exemplify the large variations of strength and diameter or distance ~~from the cloud boundaries of the subsiding shell. In some cases no subsiding shell exists at all.~~ of the downdrafts in the vicinity of the cloud boundaries. We also find ~~strong~~ updrafts or vast regions of downdrafts near the cloud~~and also frequently~~. Downdrafts are also frequent within the cloud itself, especially in the vicinity of cloud gaps (see Fig. 6 c near position 0.25).~~There are also significant updrafts outside the cloud.~~

3.2 ~~The subsiding shell in different conditions~~

~~Figures 2 b) and 5 b) show cloud examples during flight 1 with prevailing strong westerlies. Sharp gradients in the humidity profiles of the cloud transects are present at the cloud entry but on the opposite side the decrease of humidity is slower. The shape of the humidity signal is similar at different height levels but the diameter of the cloud decreases with height. It is hardly possible to identify any persisting structures in the vertical wind from one transect to the other. We found high variability of the vertical wind, especially inside the cloud, but also in its vicinity. In every transect we saw significant downdrafts. However, these downdrafts are usually not connected to the cloud boundaries, but seem to be randomly distributed. Just in some transects we found a signal similar to a subsiding shell on either side of the cloud.~~

~~The clouds sampled in flights3 to 5 developed above mountain peaks during strong high pressure influence with weak southerly wind. The convection tended to start above distinct points above the mountain ridges drifting north during its life cycle. However, in terms of downdraft regions in and near the clouds the same high variability is found as for the clouds over flat terrain.Altogether, we investigated the shell properties for 191 cloud transects based on the definition in Table 3. For this analysis a running average of $0.5\,\mathrm{sec}$ is applied to the vertical wind data to eliminate small scale turbulent fluctuations. The results are summarized in Table **??**. Only some of the investigated cloud transects (29 cases) possess a subsiding shell on both sides of the cloud. About half the cloud transects have a subsiding shell on the upwind side and approximately $30\,\%$ on the downwind or crosswind sides. The majority of the cloud transects on the downwind and crosswind sides of the cloud show a vast downdraft region near the cloud boundaries, which usually begins well within the cloud. The downdraft measured within the subsiding shell (if present) is usually not representing the absolute minimum of the vertical wind found in and around the cloud.We find 105 cloud transects with either one or two subsiding shells. We do not find an obviouscorrelation between the subsiding shell occurrences and the activity status of the clouds. There are slightly more shells found in clouds over flat terrain than over the mountains and more in the bottom and top levels compared to the mid level transects. The number of occurrences and~~ We find a similar distribution of the vertical wind also for the transects of the ~~respective cloud properties are listed in Table 4.~~ other flights. The turbulent character of the cloud environment is obvious. The up- and downdrafts seem to be rather randomly distributed with strong up- and downdrafts within the cloud as well as in the environment.

4 ~~Properties of the cumulus clouds and the subsiding shells~~

~~In the previous section we tested 191 different cloud transects on the existence of a subsiding shell. All these transects build a large sample to investigate the statistical distribution of the characteristic cloud properties. The boundaries of the clouds are estimated by the humidity distribution. Thus, the dynamical properties in the focus of the following discussion are independent of the cloud definition.~~

3.2 Distributions of wind, pressure and buoyancy

Figure 7 shows the median vertical velocity distribution for all the cloud transects. Note that the spatial coherence of the individual transects is lost with the representation of the percentiles. The median vertical velocity has a distinct maximum within the cloud, which is slightly shifted towards the upwind side. The vertical wind minimum outside of the cloud boundary is the subsiding shell. The vertical velocity becomes already negative well within the cloud. Thus, the average cloud boundary experiences downward motion. The minimum slightly outside of the cloud boundaries is stronger on the downwind side. Further away from the cloud the downdrafts become weaker. The 75 and 90 percentiles have no downdrafts at all while the 10 and 25 percentiles show continuous negative vertical velocity. The minimum near the cloud boundary is visible for all percentiles, but is weaker for the 75 and 90 percentiles.

Figure 8 shows the median vertical wind distribution for different cloud categories stratified by cloud activity, level within cloud, underlying terrain and along or crosswind transects. ~~Note that sample sizes vary.Active clouds~~ The 95 % confidence interval was computed at each point along the scaled transect by bootstrapping (1000 repetitions with replacement) and is shown in gray. Even taking the uncertainty resulting from the limited sample size into account, the median vertical velocities for all active transects in Fig. 8 a), except the bottom one, are clearly distinguishable between the interior and exterior of the cloud. Such a distinction is not possible for the inactive transects shown in Fig. 8 b), especially since even bootstrapping will underestimate the uncertainty due the smaller sample sizes for this class (Efron, 1979).

Active clouds (except at the bottom level) have pronounced updraft regions and a subsiding shell at the boundaries. The ~~minimum at the cloud boundaries is missing at the active bottom level, which might be due to the small sample available. The~~ strongest updrafts are found ~~for~~ at cloud top level. The most distinct downdraft regions at the cloud boundaries are present on the downwind side of the transects of the center level and the clouds above mountains. They have a broad region of sinking air, which already starts well within the cloud. ~~The~~ Looking at the active crosswind transects ~~show these minima as welland half a cloud diameter of the boundary the~~ we find this wind minimum as well, but here the vertical wind almost vanishes ~~. This is in contrast to the active alongwind transects . On the upwind side they~~ within half a cloud diameter. The upwind side of the active along wind transects have almost no downdrafts with a very narrow minimum right outside the cloud boundary. ~~On the downwind side the change of the vertical wind is small compared to the crosswind transects.~~ The inactive transects show high variability of the wind signals inside and outside of the cloud. At cloud mid and top level they do not show any strong updrafts.

Figure 9 shows the histograms of the vertical velocity inside the cloud and within $20\,\%$ outside of the cloud diameter. The distributions obviously differ in size and shape, with some statistical values summarized in Table 6. In the cloud the mean vertical velocity is $\approx 0.5\,\mathrm{m/s}$ and the skewness of the distribution is directly visible in the figure with increased frequencies of fast rising parcels. However, only one of the selected transects has no negative vertical velocity at all within the cloud. Except of 8 cases all the transects have downdrafts stronger than $-1\,\mathrm{m/s}$ inside the cloud. In the shell the mean vertical velocity is significantly below zero for all four cloud boundaries. Especially on the upwind side the distribution is narrow compared to the other investigated parts. In the downwind and crosswind shells we find stronger downdrafts and higher variability compared to the upwind side. The highest variability of the vertical velocity is present within the clouds, which is also visible in Fig. 7.

In Fig. 9 a) the stronger downdrafts in the downwind shell compared to the upwind shell become visible. The frequencies and magnitude of the updrafts are similar for the shell region on both sides. A separated analysis of the left and right crosswind shells does not lead to any significant differences neither for the median distributions nor for the histograms.

Figure 10 presents the median distribution of the ~~vertical mass flux~~ relative humidity and horizontal alongwind perturbation as well as the buoyancy and the horizontal pressure perturbation for the 191 selected cloud transects. The ~~vertical mass flux in panel a) is calculated with Eq. 6, which leads to a very similar distribution and magnitude as the vertical velocity. Mathematically, the vertical wind signals are weighted with the air density, which in the most cases lies near $1\,\mathrm{kg\,m^{-3}}$. Similar to the vertical wind also the vertical mass flux is continuously negative for the~~ median relative humidity within the cloud is saturated, but the 10 ~~and 25 percentiles. Also the downward directed mass flux is strongest just outside~~ percentile is significantly below. Due to the definition in Table 3 all values are $rh = 100\,\%$ at the cloud boundaries. Outside of the cloud boundaries the relative humidity decreases rapidly. The gradients are stronger on the upwind side and the median value is significantly enhanced on the downwind side for at least half a cloud diameter, which can be explained by the humidity halo on the downwind side of the cloud ~~boundaries~~(Perry and Hobbs, 1996). The mean horizontal wind component along the flight track (u_{ac}) in Fig. 10 b) is significantly reduced within the cloud, where also the strongest updrafts are found. For the 10 and 25 percentiles this signal is most pronounced. It is enhanced on the upwind side and matches the mean values on the downwind side. This feature is only present in the alongwind transects, while it is not visible in the crosswind transects. It is strongest in the bottom level transects and vanishes in the top level (not shown). The distribution of u_{ac} is also characterized by a high variability which is similar to the vertical wind variability.

Figure 10 c) shows that within the cloud a mean upward motion coincides with enhanced buoyancy, while on both sides outside of the cloud the buoyancy is almost zero on average. On the upwind side a weak negative peak is indicated with a strong and clear gradient through the cloud boundary. This gradient is much weaker on the downwind side of the cloud, where values near zero are present well within the cloud. ~~A similar feature is also visible in the relative humidity data (not shown), where the median value is significantly enhanced on the downwind side for at least half a cloud diameter.~~ The median pressure perturbation (Fig. 10 d) is small and with magnitudes of a few ~~Pascals~~ pascals similar to the sensor resolution ($= 2\,\mathrm{Pa}$). A weak negative anomaly is visible within the cloud, which is counteracted by positive contribution especially on the upwind side of the cloud. However, the percentiles show that significant deviations of the hydrostatic equilibrium are frequent both inside and outside of the clouds.

3.3 Sensitivity of the results

Even though the clouds ~~are~~ were actively chosen during the flight with a focus on vital clouds, many of them contain big cloud gaps. Different rising plumes, decaying cloud parts with strong downdrafts and also subsaturated air parcels entrained into the cloud coexist and build the entity of a single cloud. From the chosen cloud transects 9 cases have no cloud gaps at all. For 25 cases the fraction of cloud gaps relative to the cloud diameter exceeds $50\,\%$. For the 25 percentile, the median and the 75 percentile we estimate a cloud fraction of $\approx 10\,\%$, $\approx 20\,\%$ and $\approx 40\,\%$, respectively.

In order to judge the robustness of the results in terms of cloud definition, we have repeated the analyses for the stricter criteria including restriction 4 and 5 as defined in Table 3. Thus, we omit the transects with a fraction of cloud gaps of more than $30\,\%$ or a cloud gap exceeding $150\,\mathrm{m}$. For the new analysis we select the more homogeneous clouds and neglect the less active or ~~complexer~~ more complex ones, that just 94 out of 191 cloud transects remain. In Table 4 the numbers of total occurrences are listed by the numbers in brackets. ~~The frequencies of the subsiding shell remain very similar for the active transects. Just one subsiding shell is found for the inactive cases, which might be due to the small number of transects. In Figures 7 and 10 a)~~ In Figure 7 the respective median distribution for the reduced sample of 94 'ideal' clouds is represented by the green ~~lines~~line. It is obvious, that neglecting the less active clouds leads to stronger updrafts. However, the distribution at the cloud boundary and in the cloud free region remains almost unchanged. Also the histograms of the vertical velocity (not shown) remain qualitatively unchanged. The frequencies of the vertical velocities within the cloud are shifted towards higher values. The vertical velocity distribution in the shell regions are narrower compared to the results in Fig. 9. After all, the selection of the clouds ~~is not substantially changing~~ does not substantially change the results.

4 ~~Discussion~~

~~The median vertical velocity distribution around shallow convection~~

3.4 Distribution of updrafts and downdrafts

In Figure 7 we find a pattern similar to a subsiding shell on both sides of the cloud boundaries. However, due to the turbulent character of the cloudy environment the subsiding shell is not visible in most of the individual transects (as shown e.g. in Figs. 5 and 6). Instead, we find a large variety of up- and downdrafts of different strength and size inside the cloud, in the environment and also around the cloud boundaries. According to the definition in Sec. 2.3 we analysed the 191 cloud transects and found 1735 downdrafts and 1495 updrafts. This corresponds to an average of 9 different downdrafts and 8 updrafts for each cloud transect including half a cloud diameter around the clouds. Within the clouds, the average number of up- and downdrafts is approximately equal (≈ 4 of each), but the updrafts are about $25\,\%$ larger. In the environment, on the other hand, downdrafts are slightly more frequent and larger than the updrafts. Directly at the cloud boundaries, finally, the downdrafts are twice as frequent and larger as compared to the updrafts. There are only 328 up- and downdrafts in the cloud boundary region and in 56 cases no significant up- or downdraft was identified. The increased frequency of the downdrafts at the cloud boundary leads to the subsiding shell in the mean distribution of the vertical wind. A summary of the exact numbers and the main properties is given in Table 7. Most remarkably, the median sizes of the drafts are much larger directly at the cloud boundary compared to the other regions. There, also the median and variance of the vertical wind are strongest. This indicates that we find a large number of relatively small drafts within the cloud and also in the environment. These smaller drafts are less frequent at the cloud boundary which leads to the characteristic distribution shown in Fig. 11. The distributions of the drafts within the cloud and in the environment are very similar, only the frequency of large diameters is reduced in the environment. The distribution within the cloud corresponds well to the results of Yang et al. (2016). They find some larger drafts (i.e., $D > 2\,\mathrm{km}$) than in our sample, because our investigation is limited to shallow convection. The distribution at the cloud boundary is different. While at the cloud boundary the small diameters are rare, sizes of several hundred meters are most frequent for the downdrafts and somewhat larger for the updrafts. The largest of these updrafts often cover significant portions of the cloud and can form the main (i.e., the largest) updraft of the cloud. In Table 7 also the statistics for the main updrafts as a subset of the cloud updrafts are listed. These main updrafts have a median length similar to the drafts at the cloud boundary and a strength and variability of the vertical wind that is higher compared to the other categories.

The numbers of downdrafts at the cloud boundary are almost equally distributed around the cloud but they have smaller diameters at the upwind side compared to the crosswind and downwind sides as listed in Table 8. The updrafts are slightly more frequent on the upwind side. They are smallest at the crosswind side and twice as large on the downwind side. While the major parts of the downdrafts lie outside of the cloud, the updrafts are situated more inside. Table A1 in the appendix provides detailed information about the mean properties of the up- and downdrafts at the cloud border with respect to the different transect categories. A comparison of the draft diameter and median vertical velocity in the scatterplot of Fig. 12 a) shows that for all three categories larger drafts often have stronger vertical winds. For the larger diameters above $D > 200\,\mathrm{m}$ the smaller magnitudes of the vertical velocity are most often in the environment. The distribution and the high variability of the larger drafts inside the cloud and at the boundary are very similar, but the occurrences of smaller drafts at the cloud boundary is clearly reduced. In the comparison of the median vertical velocity and buoyancy in Fig. 12 b) it becomes clear that updrafts and downdrafts have both, positive and negative buoyancy and thus the median values are small. The drafts in the cloud have more cases with positive and the drafts in the environment more with negative buoyancy. However, it is clearly visible that the negative buoyancy is more frequent with downdrafts and positive buoyancy is more frequent with updrafts. The exact values are given in Table 7. There, also the correlation coefficients of the vertical velocity and buoyancy are listed. The correlation for the downdrafts is small and at the cloud boundary even slightly negative. Thus, stronger downdrafts do not necessarily have more negative buoyancy. The updrafts have a higher correlation except for the cloudfree environment.

4 Discussion

The median vertical velocity distribution presented in Fig. 7 agrees well with results of former analyses of the subsiding shell (e.g. Heus and Jonker, 2008; Wang et al., 2009; Katzwinkel et al., 2014). Different to earlier works, in the current study we considered only shallow convection over land, captured transects in all cloud levels and included also rather complex clouds (i.e, the clouds can have several updrafts and cloud holes, as long they have a common cloud base). The vertical velocity possesses a distinct minimum directly outside of the cloud boundaries, which is associated with a ~~thin~~ shell of sinking air covering the entire cloud. Figure 13 shows the relative vertical mass flux (f_m) and the relative accumulated mass flux (F_m) from the cloud center outwards. The vertical mass flux is calculated with Eq. 6, which leads to a very similar distribution and magnitude as the vertical velocity. Mathematically, the vertical wind signals are weighted with the horizontal resolution and the air density, which in the most cases lies near $1\,\mathrm{kg\,m^{-3}}$. The maximum of mass flux is found well within the cloud, while a distinct minimum exists right outside of the cloud boundary. The downward flux ~~in the shell~~ near the cloud boundary has almost the same strength as the upward flow in the main updraft region. Half of the downward mass flux along the transect occurs within a distance of 20 % of the cloud diameter outside of the cloud. After half a cloud diameter the mass flux in the cloud is compensated. Both distributions of f_m and F_m are very similar to the observations of Heus et al. (2009), even though ~~our manually selected~~ the clouds over land often have complex structures and include cloud gaps. Different ~~from~~ to their results the vertical mass flux becomes negative already well within the cloud where already a significant portion of downward mass flux occurs. This is obvious with the vertical wind distribution that becomes negative inside the cloud boundaries as well. There is no significant change in the results, when we restrict the analysis from all the 191 cases to the 130 alongwind transects as shown by the grey dashed lines in Fig. 13 or to the crosswind transects (not shown).

So far, our results corroborate the findings of ~~Heus et al. (2009)~~Heus and Jonker (2008). However, care must be taken when interpreting the mean distributions of cloud and shell properties. While a significant downdraft anomaly - the subsiding shell - is present in the median vertical wind distribution (see Fig. 7), this is not a characteristic feature of each individual cloud. ~~Only 12 cloud transect of the 94 'ideal' cases and 29 transects of the entire 191 cloud transects have the 'narrow' region of sinking air on *both* sides of~~ There is a strong variability of the vertical wind outside of the clouds and the position of the downdrafts (and also the updrafts). Although downdrafts are frequent near the cloud boundaries and also within the cloud itself, they often do not form a coherent shell around the cloud surface. Instead, these downdrafts alternate with updrafts of similar strength and diameter. The consecutive legs in Fig. 6 show how fast the wind structures change around the evolving cloud. These turbulent eddies are responsible for the vertical mass transport as well as for the entrainment of environmental air into the cloud. The presence of a subsiding shell is the result of averaging the highly variable up- and dominating downdrafts near the evolving cloud. Thus, the composition of the drafts directly at the cloud boundary form the subsiding shell. In order to understand the origin of the subsiding shell we have to look at the distribution of the up- and downdrafts. At the cloud boundary the ~~cloud. About half of the cloud transects have a subsiding shellat least at one boundary (see Table 4), even though the criteria are chosen rather generously compared to Heus and Jonker (2008). There is a strong variability~~ downdrafts are twice as frequent compared to the updrafts which leads to the characteristic distribution of the vertical wind. The downdrafts have a larger diameter at the downwind and crosswind sides, which explains the weaker signal of the subsiding shell on the upwind side. Table 8 shows that significant portions of the up- and downdrafts are situated each in and outside of the clouds~~and the position of the downdrafts (and also updrafts) . The presence of a subsiding shell depends on the current position of the downdrafts near the evolving cloud as the example~~ , which indicates the connection of the air masses to both sides of the cloud boundary. Compared to the other regions these drafts have much larger diameters, which shows the importance of the (turbulent) exchange processes at the cloud boundary. Within these up- and downdrafts, where cloudy air as well as environmental air is present, several processes are important. Most obvious is the influence due to mixing of air parcels and evaporation, but also the drag of adjacent air masses, the pressure gradient force or radiation can play a role (Park et al., 2017). Heus et al. (2009) found the evaporative cooling responsible for the subsiding shell. An indication for the evaporation at the cloud boundary is the enhanced humidity visible directly outside of the cloud in Fig. 10 a) which results very probably from evaporating cloud droplets. Same as for the downdraft velocities this effect is stronger on the downwind side of the cloud compared to the upwind side. Wang et al. (2009) and Katzwinkel et al. (2014) find the negative buoyancy near the cloud boundary as an indication for the droplet evaporation which drives the sinking shell. The results in Fig. ~~6 shows.~~ 12 and Table 7 show the same relation also for the up- and downdrafts. While most of the updrafts have positive buoyancy, it is negative for about $70\,\%$ of the downdrafts. However, the stronger downdraft does usually not indicate a lower buoyancy.

Downdrafts are frequent also inside the ~~cloud~~ clouds and have a significant influence on the mass flux. About one third of the upward directed mass flux is already compensated inside the cloud by the downdrafts. Half of these in-cloud downdrafts have a negative buoyancy and one third has significant subsaturation ($rh < 95\,\%$).

~~In the cloud, the regions of subsaturation (cloud gaps) tend to have negative vertical velocities. About $75\,\%$ of the data points in cloud gaps have a negative vertical velocity with a mean of $-0.8\,\mathrm{ms^{-1}}$. We find a positive correlation of vertical wind and buoyancy (i.e., $r \approx 40\,\%$).Near the cloud gaps this indicates mixing of cloud air with environmental air. Recently, Yang et al. (2016) also observed small scale updrafts and downdrafts as characteristic feature in isolated cumulus clouds.~~As a main conclusion from the analysed cloud transects over land, we ~~do not find either the subsiding shell nor subsidence as a characteristic feature of the vertical wind near *individual* clouds (see Fig. 6). Although downdrafts are frequent near the cloud boundaries and also within the cloud itself, they do not necessarily form a coherent shell around the cloud surface. Instead, these downdrafts often alternate with updrafts of similar strength and diameter . The consecutive legs in Fig. 6 show how fast the wind structures change around the evolving cloud . They thus resemble turbulent eddies, which can be responsible for vertical mass transport as well as entrainment of environmental air into the cloud. However,~~ find the dominating downdrafts directly at the cloud boundary to be the origin of the subsiding shell. These drafts have a median diameter of $\sim 20\,\%$ in cloud diameter (see Table 7). Defining this as the subsiding shell, its area is approximately equal to the embedded cloud. This 'subsiding shell' is a valid concept for *ensembles* of clouds as shown in Fig. 7. According to Fig. 8 ~~subsiding shells are~~ the subsiding shell is typical for active clouds, most pronounced in the center and top cloud regions or for the crosswind transects. ~~Subsiding shell are~~ The subsiding shell is more pronounced for the transects over the mountains compared to the flat land. ~~On the downwind side of active clouds the broad region of downdrafts is explainable by a humidity halo as observed by Perry and Hobbs (1996) .~~ A comparison with the results given in Table A1 shows, that for these categories the downdrafts are not more frequent and also not much stronger, but they have a larger diameter. Additionally, there is a reduced number of updrafts for the mountain, middle layer and crosswind transects compared to the transects over the land, the cloud top and alongwind. The former have much smaller diameters and weaker updrafts. Thus, the subsiding shell is not only defined by the intensity of the downdrafts, but also by the distribution and development of the updrafts at the cloud border. In Figure 8 the difference of the vertical wind distribution between the active and inactive cloud transects is striking. For the inactive transects the updraft region as well as the subsiding shell are missing. The differences of the up- and downdrafts at the cloud border of the inactive transects are less pronounced compared to the other categories. The frequency, the strength of the vertical wind and also the portion outside of the cloud (i.e., dry part) are similar. However, the variance of the vertical wind and size of the updrafts are smaller.

Our results show (see Fig. 13), that the mass transport in the cloud is compensated within half a cloud diameter away from the cloud ~~border~~boundary. This has strong implications for the distribution and mixing of the cloud air in the environment. Compared to the concept of a downward mass flux via subsidence (Stull, 1988), less mixing and less transport of heat and energy occur. The mixing of cloud air in the upper ABL is reduced when the air stays near the cloud and directly sinks down in the subsiding shell to lower regions. Thus, the 'subsiding shell' has to be considered in a parametrisation scheme for shallow convection over land.

5 Conclusions

A series of cloud transects measured with a research aircraft were analysed with a special focus on the dynamical properties near the cloud boundaries. Former LES model results had shown a narrow coating downdraft region around shallow convective clouds, which is called a subsiding shell.

To test whether ~~subsiding shells~~ the subsiding shell can be observed for shallow convection over land, we conducted 6 measurement flights in the years 2012 and 2013. It was possible to probe single clouds over flat land and mountain ridges, in different heights and different synoptic situations. The aircraft measured the thermodynamic properties of the clouds with the exception of liquid water content. A correction is presented for the temperature and humidity bias that occurs due to droplet evaporation inside the clouds. The target clouds were actively selected during the flights in order to choose well-defined vital clouds. For the investigation we manually selected 191 cloud transects. The clouds are usually not homogeneous masses of cloud air with a central main updraft but more complex formations with regions of updrafts, downdrafts and cloud gaps within one cloud. With a stricter cloud definition we repeated the analysis with a reduced cloud sample of 94 'ideal' clouds for a sensitivity test. The median vertical velocity of the selected cloud transects shows a very similar distribution compared to the LES model results. We also do not see any significant differences between our measurements over land surface compared to earlier results from shallow convection over sea. The main feature in the distribution is a distinct minimum in the vertical wind immediately outside of the cloud boundaries. A distinct downdraft on the downwind side starts well within the cloud and is wider compared to the upwind side, where the gradients of vertical velocity and buoyancy are stronger. A strong downward mass flux is present in the region of the subsiding shell, which compensates for a large fraction of the positive vertical mass transport within the cloud. Within a distance outside the cloud of $\approx 20\,\%$ in cloud diameter half of the upward directed vertical mass flux is compensated.

~~On the other hand, individual cloud transects do not usually possess a subsiding shell as defined in Table 3. Just 29 of the 191 investigated cloud transects have a subsiding shell on both boundaries and 105 transects on at least one side.~~ In general, the distribution of the vertical wind is qualitatively similar over flat land and mountainous terrain, but there are quantitative differences. Active clouds have larger vertical velocity and vertical mass flux than inactive clouds. The strongest updrafts are present in the upper level and crosswind transects, while the downdrafts are most pronounced at the center level and mountain transects.

Due to the turbulence in the environment of the clouds, the subsiding shell is not visible in the individual cloud transects. Strong downdrafts are twice as frequent in the vicinity of the cloud boundaries compared to the updrafts, which leads to the characteristic feature of a subsiding shell in the mean vertical velocity profile. The individual cloud transects are characterized by strong updrafts and downdrafts both, inside and outside the cloud. They seem rather randomly distributed ~~and resemble turbulent eddies , which are~~ which is expectable for turbulent eddies with sizes much smaller than the cloud diameter. ~~An investigation~~

~~of size, turbulence statistics and scaling with~~ Compared to the cloud and the environment the diameters of the ~~cloud size in future research is desirable to understand the dynamics of shallow convection over land. Still, the~~ up- and downdrafts at the cloud boundary are much larger with stronger and more variable vertical wind. Only the strongest updrafts inside of each cloud lead to a similar distribution of size and strength. The drafts at the cloud boundary have a median diameter of $\sim 20\,\%$ in cloud diameter and form the subsiding shell. In the middle layer, above the mountains and crosswind the downdrafts have the largest diameters, they are strongest at the cloud tops and above the mountains. The striking difference of the vertical wind distribution between the active and inactive cloud transects (i.e., the inactive clouds do not show a distinct updraft region nor the subsiding shell) is not directly visible for the up- and downdrafts at the cloud border. The majority of the downdrafts at the cloud boundary have negative buoyancy and the relative humidity is increased compared to the cloudfree environment, which both indicates the importance of evaporative cooling for the formation of the subsiding shell. However, the reason for the dominating sizes of the drafts directly at the cloud boundary cannot yet be explained and remains an open question for future research. Finally, the concept of the subsiding shell seems a valid concept for mean properties of shallow convection over land with all its implications on the cloud air mixing and entrainment of upper level air into the cloud. The downdraft in the subsiding shell is able to account for a major part of the downward mass flux, which is compensating the net upward mass flux in the cloud. In contrast to subsidence in a large area between the clouds this process reduces the horizontal mixing of cloud air in the upper boundary layer, but keeps the cloud air in the near vicinity of the cloud itself.

Data availability. Data on personal request

Competing interests. All authors declare that they have no competing interests.

Acknowledgements. We thank the DLR flight crew for their enthusiastic commitment while circling in narrow turns around the target clouds. We thank the air traffic authorities in Germany and Austria for their support, which gave the permission to freely sample the clouds in these regions of high air traffic. Furthermore, we thank the two anonymous reviewers for their insightful comments which largely improved the paper.

Appendix: Characteristics of up- and downdrafts at the cloud border

Table A1 is an expansion of Table 7. It contains the detailed information of the up- and downdrafts at the cloud border separately for the different transect categories.

References

Abma, D., Heus, T., and Mellado, J. P.: Direct Numerical Simulation of Evaporative Cooling at the Lateral Boundary of Shallow Cumulus Clouds, J. Atmos. Sci., 70, 2088–2102, http://dx.doi.org/10.1175/JAS-D-12-0230.1, 2013.

Bange, J., Beyrich, F., and Engelbart, D. A. M.: Airborne measurements of turbulent fluxes during LITFASS-98: Comparison with ground measurements and remote sensing in a case study, Theoretical and Applied Climatology, 73, 35–51, http://dx.doi.org/10.1007/s00704-002-0692-6, 2002.

Blyth, A. M., Lasher-Trapp, S. G., and Cooper, W. A.: A study of thermals in cumulus clouds, Quarterly Journal of the Royal Meteorological Society, 131, 1171–1190, http://dx.doi.org/10.1256/qj.03.180, 2005.

Buck, A. L.: the variable-path Lyman-alpha hygrometer and its operating characteristics, Bull. Amer. Meteor. Soc., 57, 1113–1119, https://doi.org/10.1175/1520-0477(1976)057<1113:tvplah>2.0.co;2, https://doi.org/10.1175/1520-0477(1976)057<1113:TVPLAH>2.0.CO;2, 1976.

Efron, B.: Bootstrap Methods: Another Look at the Jackknife, Ann. Statist., 7, 1–26, https://projecteuclid.org:443/euclid.aos/1176344552, 1979.

Heus, T. and Jonker, H. J. J.: Subsiding Shells around Shallow Cumulus Clouds, J. Atmos. Sci., 65, 1003–1018, http://dx.doi.org/10.1175/2007JAS2322.1, 2008.

Heus, T., J. Pols, C. F., J. Jonker, H. J., A. Van den Akker, H. E., and H. Lenschow, D.: Observational validation of the compensating mass flux through the shell around cumulus clouds, Quarterly Journal of the Royal Meteorological Society, 135, 101–112, http://dx.doi.org/10.1002/qj.358, 2009.

Houze, R. A. J.: Cloud Dynamics, vol. 104, Academic Press, 2nd edition edn., 2014.

Jonas, P.: Observations of cumulus cloud entrainment, Atmospheric Research, 25, 105 – 127, http://dx.doi.org/10.1016/0169-8095(90)90008-Z, 1990.

Jonker, H. J. J., Heus, T., and Sullivan, P. P.: A refined view of vertical mass transport by cumulus convection, Geophys. Res. Lett., 35, L07 810–, http://dx.doi.org/10.1029/2007GL032606, 2008.

Katzwinkel, J., Siebert, H., Heus, T., and Shaw, R. A.: Measurements of Turbulent Mixing and Subsiding Shells in Trade Wind Cumuli, J. Atmos. Sci., 71, 2810–2822, http://dx.doi.org/10.1175/JAS-D-13-0222.1, 2014.

Lawson, R. P. and Cooper, W. A.: Performance of Some Airborne Thermometers in Clouds, J. Atmos. Oceanic Technol., 7, 480–494, http://dx.doi.org/10.1175/1520-0426(1990)007<0480:POSATI>2.0.CO;2, 1990.

Mallaun, C. and Giez, A.: The Missing Link: How to optimize pressure calibration using the tower flyby method, in: 24th Annual SFTE EC Symposium, http://elib.dlr.de/95001/, 2013.

Mallaun, C., Giez, A., and Baumann, R.: Calibration of 3-D wind measurements on a single-engine research aircraft, Atmospheric Measurement Techniques, 8, 3177–3196, https://www.atmos-meas-tech.net/8/3177/2015/amt-8-3177-2015.pdfDO-10.5194/amt-8-3177-2015ER-, 2015.

Park, S.-B., Heus, T., and Gentine, P.: Role of convective mixing and evaporative cooling in shallow convection, Journal of Geophysical Research: Atmospheres, 122, 5351–5363, https://agupubs.onlinelibrary.wiley.com/doi/abs/10.1002/2017JD026466, 2017.

Perry, K. D. and Hobbs, P. V.: Influences of Isolated Cumulus Clouds on the Humidity of Their Surroundings, J. Atmos. Sci., 53, 159–174, http://dx.doi.org/10.1175/1520-0469(1996)053<0159:IOICCO>2.0.CO;2, 1996.

Rodts, S. M. A., Duynkerke, P. G., and Jonker, H. J. J.: Size Distributions and Dynamical Properties of Shallow Cumulus Clouds from Aircraft Observations and Satellite Data, J. Atmos. Sci., 60, 1895–1912, http://dx.doi.org/10.1175/1520-0469(2003)060<1895:SDADPO>2.0.CO;2, 2003.

Schmeissner, T., Shaw, R. A., Ditas, J., Stratmann, F., Wendisch, M., and Siebert, H.: Turbulent Mixing in Shallow Trade Wind Cumuli: Dependence on Cloud Life Cycle, J. Atmos. Sci., 72, 1447–1465, https://doi.org/10.1175/JAS-D-14-0230.1, http://dx.doi.org/10.1175/JAS-D-14-0230.1, 2015.

Scorer, R. S. and Ludlam, F. H.: Bubble theory of penetrative convection, Quarterly Journal of the Royal Meteorological Society, 79, 94–103, http://dx.doi.org/10.1002/qj.49707933908, 1953.

Stull, R. B.: An introduction to Boundary Layer Meteorology, Kluwer Academic Publishers, 1988.

Stull, R. B.: Meteorology for Scientists and Engineers, Brooks/Cole, 2 edn., 2000.

Wang, Y. and Geerts, B.: Humidity variations across the edge of trade wind cumuli: Observations and dynamical implications, Atmospheric Research, 97, 144 – 156, http://dx.doi.org/10.1016/j.atmosres.2010.03.017, 2010.

Wang, Y., Geerts, B., and French, J.: Dynamics of the Cumulus Cloud Margin: An Observational Study, J. Atmos. Sci., 66, 3660–3677, http://dx.doi.org/10.1175/2009JAS3129.1, 2009.

Warner, J.: Time Variation of Updraft and Water Content in Small Cumulus Clouds, J. Atmos. Sci., 34, 1306–1312, https://doi.org/10.1175/1520-0469(1977)034<1306:TVOUAW>2.0.CO;2, http://dx.doi.org/10.1175/1520-0469(1977)034<1306:TVOUAW>2.0.CO;2, 1977.

Yang, J., Wang, Z., Heymsfield, A. J., and French, J. R.: Characteristics of vertical air motion in isolated convective clouds, Atmospheric Chemistry and Physics, 16, 10 159–10 173, http://www.atmos-chem-phys.net/16/10159/2016/, 2016.

~~Examples of clouds in weak and strong shear environments, respectively. (a) Cloud in weak-wind, weak-shear environment during flight 2. Common cloud base in a humid surrounding with $rh > 85\,\%$, but cloud gaps in the upper part, which is surrounded by drier air $rh \approx 60\,\%$. Weak winds blow in the lower cloud part with $\approx 2-4\,\mathrm{ms}^{-1}$, the inclination of the cloud top indicates increasing wind with height. (b) Cloud in a boundary layer with strong wind shear during flight 1 immediately before a crosswind transect. The wind blows from the left and the shear-induced declination of the cloud is visible. The cloud bottom does not show a sharp line, which indicates that the cloud has reached at least a mature state, without a strong updraft in the lower cloud parts.~~

~~Distribution of sizes of the downdrafts just outside of the clouds for the 191 cloud transects. The left and right sides of the 61 crosswind transects are considered together. The percentages are measured relative to the cloud diameter. Only 29 cloud transects have a subsiding shell fulfilling the criteria in Table 3 on both sides and about half the transects have at least one subsiding shell.shell downdraft no near downdraft $1-20\,\%$ $>20\,\%$ downdraft in cloud $>20\,\%$upwind 59 4319 9 downwind 39 58 23 10 crosswind 36 69 13 4~~

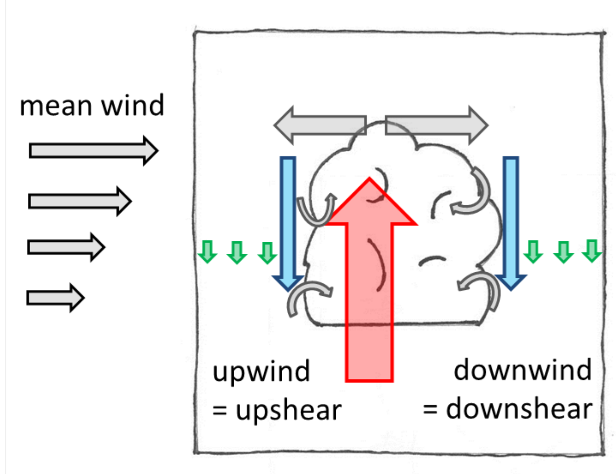

Figure 1. Conceptual model of a small cumulus cloud. The vertical mass flux within the cloud (red arrow) is compensated either through large scale subsidence (green arrows) or in the subsiding shell (blue arrows). Grey arrows indicate detrainment above the cloud and entrainment on the lateral cloud boundaries.The main updraft is shifted towards the upshear cloud boundary.

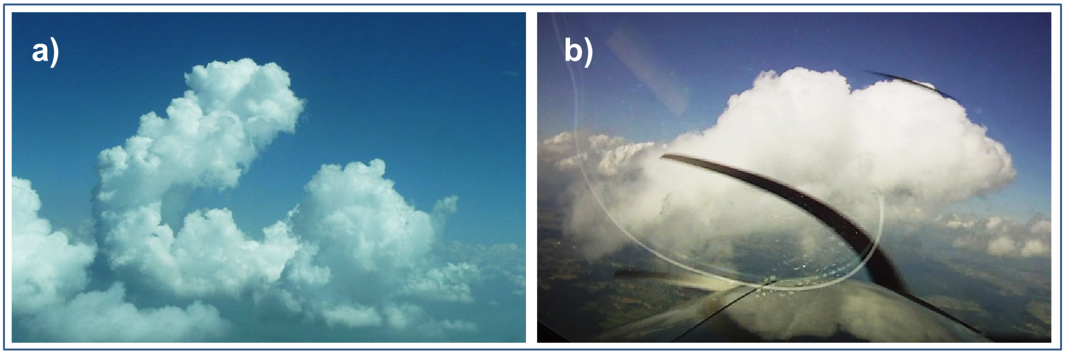

Figure 2. Examples of clouds in weak and strong shear environments, respectively. (a) Cloud in weak-wind, weak-shear environment during flight 2. It has a common cloud base, but cloud gaps in the upper part, which is surrounded by drier air $rh \approx 60\,\%$. Weak winds blow in the lower cloud part with $\approx 2-4\,\mathrm{ms}^{-1}$, the inclination of the cloud top indicates increasing wind with height. (b) Cloud in a boundary layer with strong wind shear during flight 1 immediately before a crosswind transect. The wind blows from the left and the shear-induced declination of the cloud is visible. The cloud bottom does not show a sharp line, which indicates that the cloud has reached at least a mature state, without a strong updraft in the lower cloud parts.

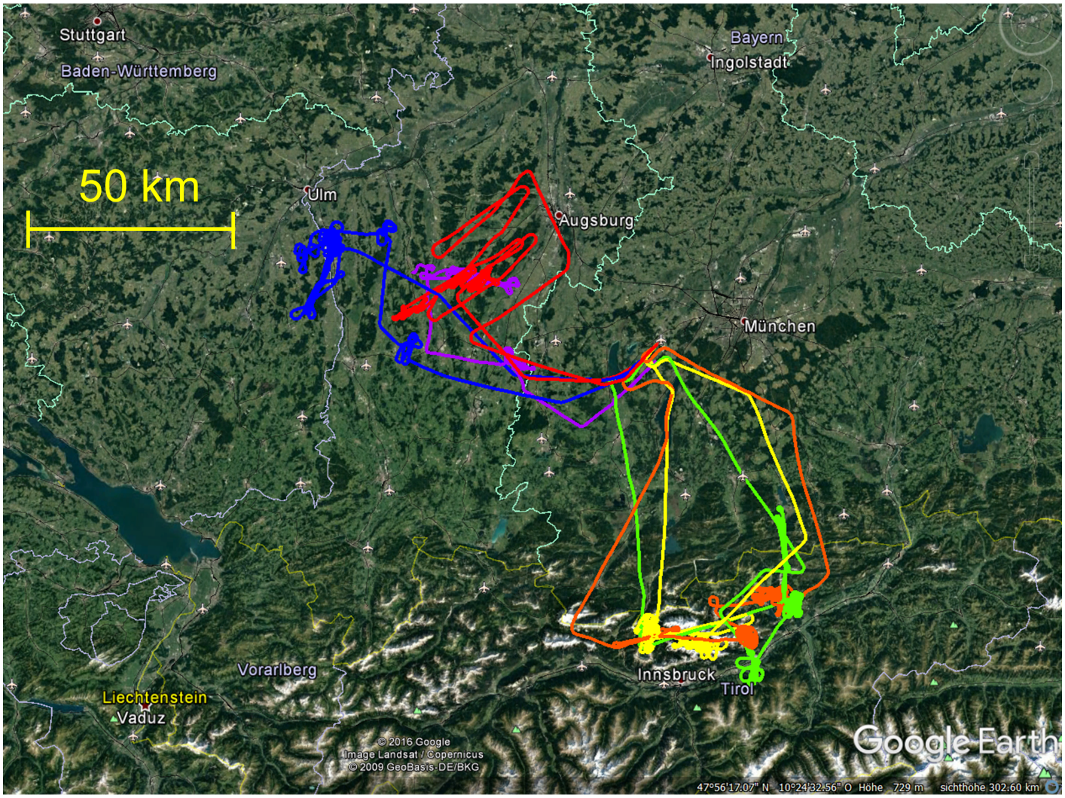

Figure 3. Overview of the target region for the measurement flights above the northern Limestone Alps and foothills west of Munich. The lines show the 6 flights listed in Table 2 colored blue, red, orange, yellow, green and purple, respectively. The thin yellow line marks the border between Austria and Germany (2016 Google, Image Landsat / Copernicus).

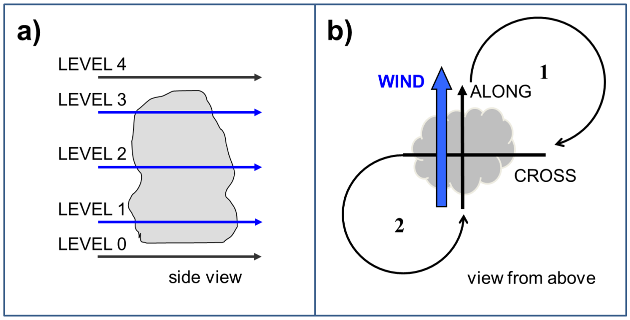

Figure 4. Definition of the chosen levels (a) and directions (b) during the measurement flights. The turns 1 and 2 in panel (b) indicate the main flight pattern resembling the number '8', which results in repeated flight transects along and cross the mean wind.

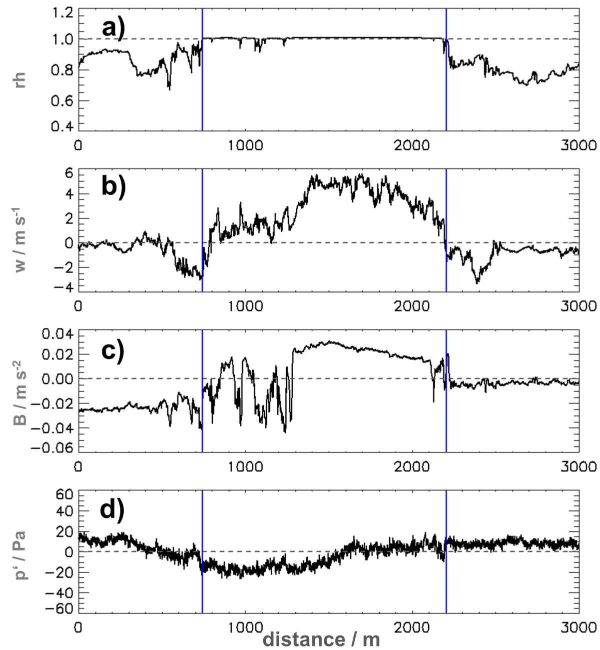

Figure 5. ~~a)~~ Measurement values for a crosswind transect through an active cloud during flight 2 looking downwind. The cloud boundaries are marked by the ~~grey~~ blue vertical lines. Panel (~~i~~a) shows relative humidity; (~~ii~~b) vertical wind; (~~iii~~c) buoyancy ~~based on a mean LWC of $0.4\,\mathrm{gm}^{-3}$, the blue line is buoyancy~~ without the contribution of LWC and (~~iv~~d) the horizontal pressure perturbation. ~~b) Same for an alongwind transect during flight 1.~~

Table 1. List of the measurement uncertainties for the main meteorological parameters of the sensors flown on the Caravan research aircraft. Results from Mallaun and Giez (2013)

Quantity	Variable	σ
Static air temperature	ts	$0.15\,\mathrm{K}$ ($0.5\,\mathrm{K}$ in clouds)
Humidity mixing ratio	mr	$2\,\%$($4\,\%$ below $0.5\,\mathrm{g/kg}$)
Relative humidity	rh	$3\,\%\mathrm{rh}$($5\,\%\mathrm{rh}$ below $0.5\,\mathrm{g/kg}$)
Dewpoint temperature	T_d	$0.35\,\mathrm{K}$ ($0.5\,\mathrm{K}$ in clouds)
Angle of attack	α	$0.25°$
Angle of sideslip	β	$0.25°$
Wind speed	ws	$0.3\,\mathrm{m/s}$
Wind angle	wa	$2°$
Alongwind component	u_f	$0.3\,\mathrm{m/s}$
Crosswind component	v_f	$0.3\,\mathrm{m/s}$
Vertical wind	w	$0.25\,\mathrm{m/s}$

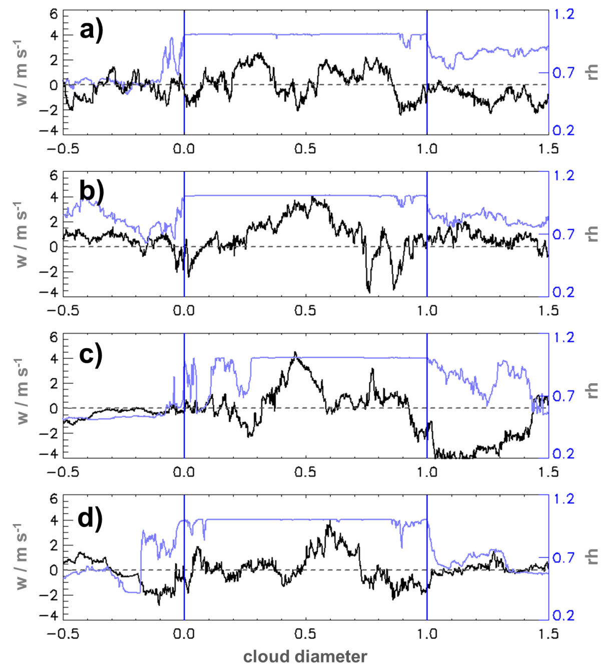

Figure 6. Relative humidity (blue line) and vertical wind (black line) for four alongwind directed cloud transects of an individual cloud during flight 2. The blue vertical lines indicate the cloud boundaries. The x-axis is scaled to the horizontal diameter of the cloud, where 0 marks the cloud edge on the upwind side and 1 the downwind edge. The data outside the cloud are shown for half a cloud diameter, each. The starttime of the transect, cloud length and height of the flight level are for panel (a) 12.27 UTC, 1043 m and 2620 m a.s.l., panel (b) 12.33 UTC, 1561 m and 2620 m a.s.l., panel (c) 12.40 UTC, 772 m and 2920 m a.s.l., panel (d) 12.42 UTC , 673 m and 2940 m a.s.l..

Table 2. Summary of flights conducted during the measurement campaigns in June 2012 and July 2013, with the number of cloud transects used in this study (191 total) and their pressure height measured in hecto feet. The given values for the environmental air correspond to the lowest and highest flight level, respectively. The lifted condensation level (LCL) is estimated with the Henning equation (e.g., Schmeissner et al., 2015) from the profile data measured during takeoff and landing at the airport about 80 km north of the target area.

number	date	time [UTC]	number of transects	flight levels [hft]	temperature [°C]	wind [ms^{-1}]	relative humidity	LCL [m]
1	10/07/2012	12:30 – 14:58	38	75, 80, 90	7 – 3	10 – 16	85 – 80	2050
2	26/07/2012	8:15 – 10:45	47	70, 80, 90	11 – 5	2 – 4,	70 – 55	2100
3	18/06/2013	11:20 – 14:10	30	115, 120, 130	4 – 0	4 – 6	65 – 40	3050
4	19/06/2013	11:29 – 14:15	35	120, 130	3 – 0	8 – 10	60 – 50	3250
5	20/06/2013	11:26 – 14:08	22	120, 130	3 – 0	6 – 6	60 – 50	2600
6	26/06/2013	9:00 – 11:36	19	60	−1	7	75	1400

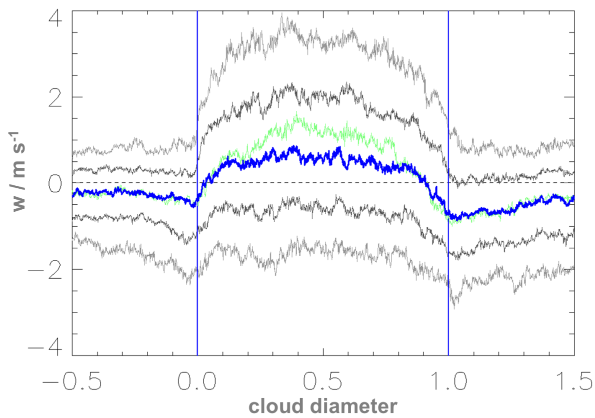

Figure 7. Distribution of the vertical wind speed of 191 cloud transects: median (blue line) $10, 25, 75$ and 90 percentiles (grey lines) with the scaling of the x-axis and the cloud boundaries as in Fig. 6. The individual cloud transects are scaled by the cloud length. The transects are arranged in a way that the upwind side is on the left and the crosswind transects are shown from left to right. The vertical blue lines indicate the cloud boundaries. The green solid line is the median of the vertical wind velocity for 94 selected cloud transects, which fulfill the stricter cloud requirements in Table 3.

Table 3. Criteria for identifying the cloud~~and the subsiding shell~~. The stricter cloud requirements 4 and 5 are optional and used in a repetition of the analysis in order to test the sensitivity of the results.

	Cloud criteria:
1.	The cloud boundaries are defined by reaching humidity saturation.
2.	A cloud has a minimum diameter of $200\,\mathrm{m}$.
3.	All parts of a single cloud possess a common cloud base,
	thus, a cloud transect can also contain regions of subsaturation (cloud gaps)
(4.	Any region of subsaturation (cloud gap) is shorter than $150\,\mathrm{m}$.)
(5.	The cloud gaps may not cover more than $30\,\%$ of the cloud diameter)
~~Minimum criteria for a subsiding shell:...~~	

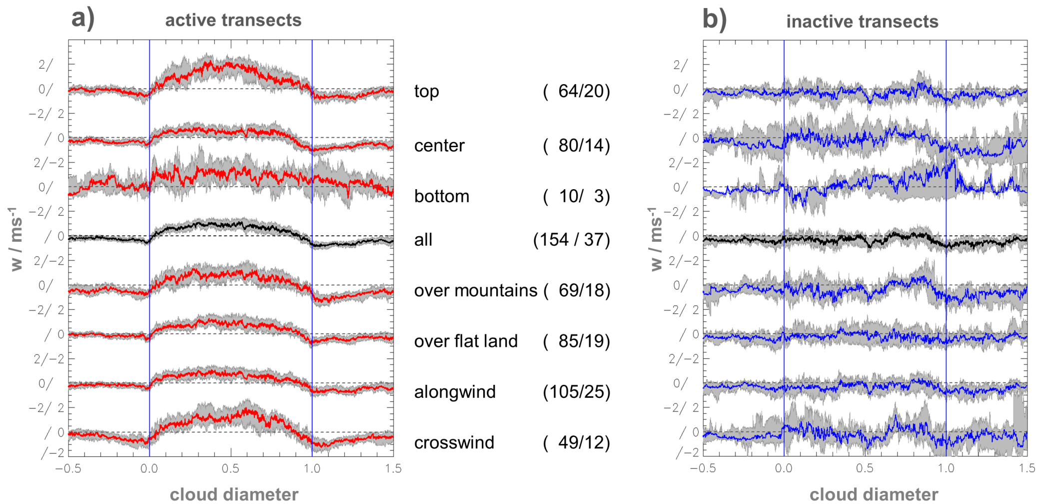

Figure 8. a) Median of the vertical wind for different transect heights, terrain, direction ~~and activity status~~for the active cloud transects. The comparison is based on the 191 cloud transects shown in Fig. 7, with the same scaling of the x-axis. The red lines show active ~~and the blue lines dissolving~~ clouds. The detailed selection is explained ~~on~~ in between the ~~right hand side~~ two panels of the respective line including the number of involved cases (i.e., active / inactive cases). For better readability the lines are vertically shifted and the grey dashed horizontal lines show the different 0 lines. Two adjacent 0 lines are separated by ~~$2\,\mathrm{ms}^{-1}$~~$4\,\mathrm{ms}^{-1}$. In order to show the statistical significance of the transect samples a statistical resampling (bootstrapping method) with 1000 repetitions is performed. The resulting spread of the 95 % confidence interval for each is transect category is shown by the grey shaded area. b) same for the inactive transects (blue lines).

Table 4. Characteristics of the 191 (94) selected cloud transects as defined in Table 3. Numbers in parentheses are relative to the subset of 94 clouds with stricter limits on the cloud gaps. The transects are divided into legs along and cross to the main wind direction, into legs at the bottom, center or top of the cloud and the activity status. Active clouds have a positive mean buoyancy inside the cloud.~~Total numbers of cloud transects and transects which fulfill the criteria of a subsiding shell are listed.~~

	along	cross	flat land		mountain	
			active	inactive	active	inactive
total	130 (60)	61 (34)	85 (49)	19 (6)	68 (37)	19 (2)
~~shell …~~						
	bottom		center		top	
	active	inactive	active	inactive	active	inactive
total	10 (8)	3 (2)	80 (47)	14 (5)	63 (31)	21 (1)
~~shell …~~						

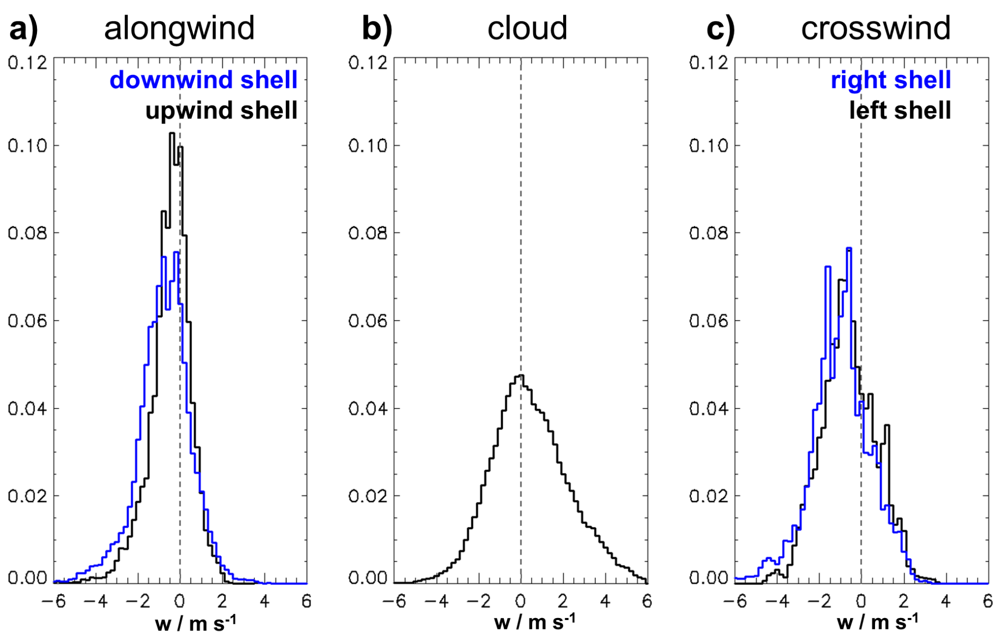

Figure 9. Distribution of the vertical wind in the cloud and shell regions for the 191 cloud transects. The three panels show the probability density function for a) the upwind shell and the downwind shell; b) the cloud and c) the right shell /left shell for the crosswind transects. For the distribution we set a bin size of $0.2\,\mathrm{m\,s^{-1}}$ and the results are scaled with the number of data points. The width of each shell is set to $20\,\%$ of the respective cloud diameter.

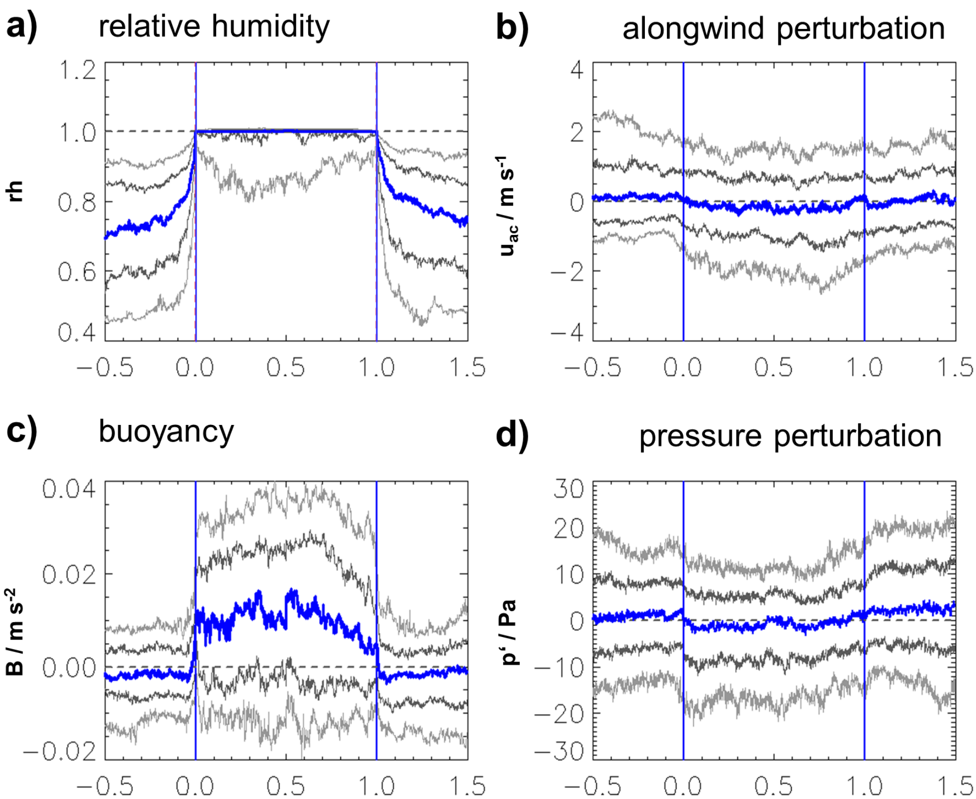

Figure 10. Same as Fig. 7 for the ~~vertical mass flux~~ relative humidity (a), horizontal wind perturbation of the along flight path component (b), buoyancy (c) and the horizontal pressure perturbation (d). ~~The red line in panel (c) is the median buoyancy calculated without the negative contribution of the LWC.~~

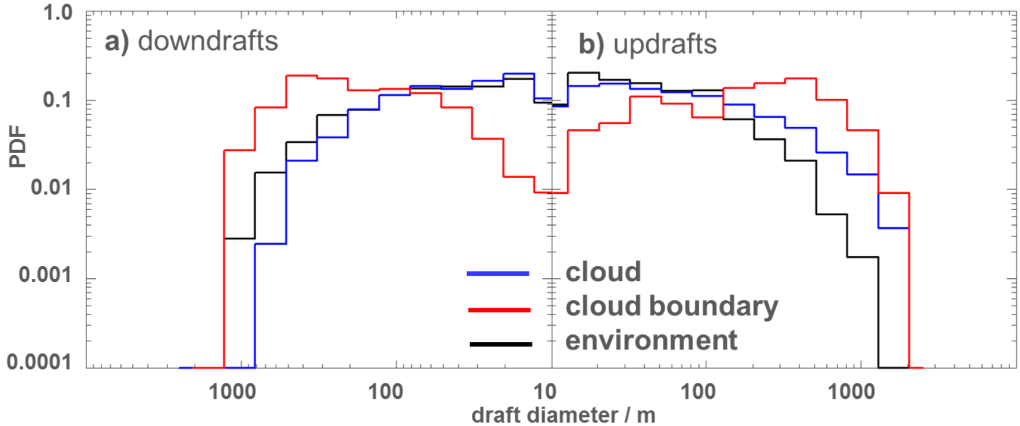

Figure 11. ~~(a) Mean vertical mass flux (f_m) along 191 cloud transects scaled with~~ PDFs of the ~~maximum mass flux. The x-axis is scaled with~~ diameters of the ~~cloud diameter~~updrafts and downdrafts. The ~~grey dashed line shows the scaled f_m~~ distributions are shown separately for ~~130 alongwind transects. (b) Integrated mass flux (F_m) from~~ the ~~center~~ drafts inside of the cloud~~(i.e.~~, ~~Eq. 7) scaled with~~ at the ~~maximum value~~cloud boundaries and the near environment.

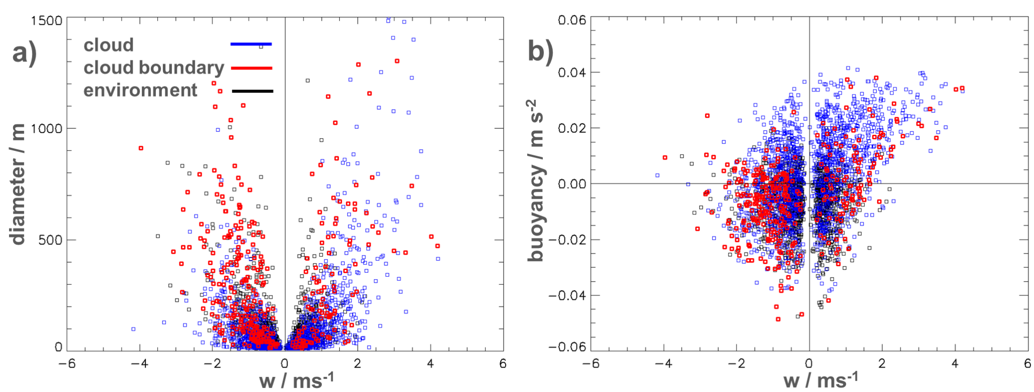

Figure 12. a) Scatterplot of median vertical velocities (w) and diameters for the up- and downdrafts in the cloud, at the cloud boundary and the environment. Each point represents one individual draft. b) Same for the median vertical velocities (w) and buoyancy.

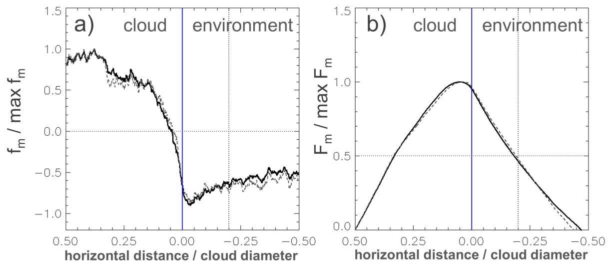

Figure 13. (a) Mean vertical mass flux (f_m) along 191 cloud transects scaled with the maximum mass flux. The x-axis is scaled with the cloud diameter. The grey dashed line shows the scaled f_m for 130 alongwind transects. (b) Integrated mass flux (F_m) from the center of the cloud (i.e., Eq. 7) scaled with the maximum value. The dotted vertical line in both panels indicates the position of 20 % in cloud diameter where ≈ 50 % of the upward massflux is compensated by the subsiding shell.

Table 5. Change of saturation dewpoint temperature in dependence of water vapor mixing ratio for different dewpoint temperatures (TS) and pressures (PS) during the measurement flights. The last column gives the estimated average value which is used for the temperature correction described in Sect. 2.4

flight	FL [hft]	PS [hPa]	TS [°C]	$\frac{\partial T_d}{\partial r}$ [K g^{-1}kg]	$\overline{\frac{\partial T_d}{\partial r}}$
	75	770	7	1.8	
1	85	735	5	1.9	2.0
	95	705	2	2.2	
	75	770	10	1.5	
2	85	735	8	1.6	1.6
	100	700	5	1.8	
	125	630	5	1.6	
3-5	130	625	4	1.7	1.8
	140	595	1	2.0	
6	65	800	2	2.5	2.5

Table 6. Vertical wind speeds [$\mathrm{ms^{-1}}$] of 191 selected cloud transects. The length of the cloud interior is variable and the shells are limited to 20 % of the cloud diameter. The table shows the mean vertical velocities, the median as well as the 25 and 75 percentiles.

	mean	25 percentile	median	75 percentile
cloud	+0.5	−0.7	+0.4	+1.7
upwind shell	−0.4	−0.9	−0.3	+0.2
downwind shell	−0.7	−1.4	−0.6	+0.1
crosswind shell	−0.8	−1.6	−0.7	+0.2

Table 7. Numbers and median properties of the downdrafts and updrafts selected from the 191 cloud transects according to the definition in Sec. 2.3. The drafts inside the cloud, at the cloud boundary and in the environment are investigated separately. The median value is listed for the absolute length and relative to the cloud diameter (rel. length), the vertical velocities and the variance of the vertical velocity. This is followed by the fraction of positive buoyancy ($B > 0\,\mathrm{ms^{-2}}$) and finally the correlation coefficient (r_{wB}) of buoyancy and vertical wind.

		numbers	length [m]	rel. length [%]	vertical wind [$\mathrm{ms^{-1}}$]	variance [$\mathrm{m^2s^{-2}}$]	$B > 0\,\mathrm{ms^{-2}}$ [%]	r_{wB}
downdrafts	all	1735	58	4	−0.7	0.10	34	0.03
	cloud	810	46	3	−0.7	0.11	42	0.12
	cloud border	217	223	19	−1.1	0.28	29	−0.22
	environment	708	52	4	−0.5	0.05	25	−0.02
updrafts	all	1495	57	4	0.6	0.09	52	0.48
	cloud	813	58	4	0.7	0.16	71	0.44
	cloud border	109	233	17	1.1	0.32	55	0.54
	environment	573	45	3	0.4	0.04	24	0.08
	cloud main updraft	179	290	24	1.5	0.5	88	0.55

Table 8. Number, median length and median relative portion of the drafts outside of the cloud (dry part) for the drafts at the cloud border. Subsets are shown for the drafts on the upwind, downwind and crosswind sides of the cloud.

downdrafts	numbers	length [m]	dry part [%]
upwind	69	155	75
downwind	76	240	57
crosswind	72	287	73
updrafts			
upwind	43	201	31
downwind	35	347	35
crosswind	31	159	42

Table A1. Similar Table 7 but for the different transect categories at the cloud border. The last two columns are missing, instead the portion of the dry part as in Table 8 is listed.

		numbers transects	numbers drafts	length [m]	rel. length [%]	vertical wind [ms^{-1}]	variance	dry part [%]
downdrafts	cloud border all	191	217	223	19	-1.1	0.28	69
	top	64	71	191	18	-1.3	0.35	79
	middle	80	91	254	20	-1.1	0.25	62
	bottom	10	8	100	8	-0.7	0.18	78
	land	85	98	184	17	-1.0	0.25	66
	mountain	69	72	341	31	-1.2	0.37	75
	along	105	112	187	17	-1.1	0.27	67
	cross	49	58	287	27	-1.2	0.35	77
	all inactive	37	47	273	19	-1.1	0.24	61
updrafts	cloud border all	191	109	233	17	1.1	0.32	35
	top	64	38	181	22	1.2	0.50	39
	middle	80	40	270	22	1.2	0.31	24
	bottom	10	11	360	23	0.8	0.22	62
	land	85	54	290	24	1.2	0.33	29
	mountain	69	35	172	15	1.0	0.33	42
	along	105	662	270	18	1.2	0.33	36
	cross	49	23	233	18	1.1	0.41	42
	all inactive	37	20	95	8	1.1	0.23	35